Chandra Deep Field South: The 1Msec Catalog

Riccardo Giacconi[1,2], Andrew Zirm[1], JunXian Wang[1], Piero Rosati[3], Mario Nonino[4], Paolo Tozzi[4], Roberto Gilli[1,5], Vincenzo Mainieri [3,6], Guenther Hasinger[7], Lisa Kewley[8], Jacqueline Bergeron[3], Stefano Borgani[9], Roberto Gilmozzi[3], Norman Grogin [10], Anton Koekemoer[10], Ethan Schreier[10], Wei Zheng[1] and Colin Norman[1,10]

ABSTRACT

In this Paper we present the source catalog obtained from a 942 ks exposure of the *Chandra* Deep Field South (CDFS), using the Advanced CCD Imaging Spectrometer (ACIS–I) on the *Chandra* X–ray Observatory. Eleven individual pointings made between October 1999 and December 2000 were combined to generate the final image used for object detection. Catalog generation proceeded simultaneously using two different methods; a method of our own design using a modified version of the `SExtractor` algorithm, and a wavelet transform technique developed specifically for *Chandra* observations. The detection threshold has been set in order to have less than 10 spurious sources, as assessed by extensive simulations. We subdivided the catalog into four sections. The primary list consists of objects common to the two detection methods. Two secondary lists contain sources which were detected by: 1) the `SExtractor` algorithm alone and 2) the wavelet technique alone. The fourth list consists of possible diffuse or extended sources. The flux limits at the aimpoint for the soft (0.5–2 keV) and

[1]The Johns Hopkins University, Homewood Campus, Baltimore, MD 21218

[2]Associated Universities, Inc. 1400 16th Stret, NW, Suite 730, Washington, DC 20036

[3]European Southern Observatory, Karl-Schwarzschild-Strasse 2, Garching, D-85748, Germany

[4]Osservatorio Astronomico, Via G. Tiepolo 11, 34131 Trieste, Italy

[5]Osservatorio Astrofisico di Arcetri, Largo E. Fermi 5, I-50125 Firenze, Italy

[6]Dipartimento di Fisica "E.Amaldi", Universitá degli Studi RomaTre, Via della Vasca Navale 84, I-00146 Roma, Italy

[7]Astrophysikalisches Institute Potsdam, An der Sternwarte 16, Potsdam, D-14482, Germany

[9]Harvard Smithsonian Center for Astrophysics, 60 Garden Street, Cambridge, MA 02138

[9]INFN, c/o Dip. di Astronomia dell'Università, via Tiepolo 11, I–34131, Trieste, italy

[10]Space Telescope Science Institute, 3700 San Martin Drive, Baltimore, MD 21218

hard (2–10 keV) bands are 5.5×10^{-17} erg s^{-1} cm^{-2} and 4.5×10^{-16} erg s^{-1} cm^{-2} respectively. The total number of sources is 346; out of them, 307 were detected in the 0.5–2 keV band, and 251 in the 2–10 keV band.

We also present optical identifications for the catalogued sources. Our primary optical data is R band imaging from VLT/FORS1 to a depth of $R \sim 26.5$ (Vega). In regions of the field not covered by the VLT/FORS1 deep imaging, we use R–band data obtained with the Wide Field Imager (WFI) on the ESO–MPI 2.2m, as part of the ESO Imaging Survey (EIS), which covers the entire X–ray survey. We found that the FORS1/Chandra offsets are small, $\sim 1''$. Coordinate cross-correlation finds 85% of the *Chandra* sources covered by FORS1 R to have counterparts within the 3σ error box ($\gtrsim 1.5''$ depending on off–axis angle and signal–to–noise). The unidentified fraction of sources, approximately $\sim$ 10–15%, is close to the limit expected from the observed X–ray flux to R–band ratio distribution for the identified sample.

1. Introduction

The X–ray background (hereafter XRB) was first identified by Giacconi et al. (1962) and its resolution into discrete sources has since been a major goal of X–ray astronomy. Deep surveys by the major X–ray facilities UHURU (Matilsky et al. 1973), HEAO-1 A2 (Piccinotti et al. 1982), Einstein (Giacconi et al. 1979), ROSAT (Hasinger et al. 1998), ASCA (Ueda et al. 1999) and BeppoSAX (Giommi et al. 2000) have resolved an increasing fraction of the XRB in the 0.5–2 keV and in the 2–7 keV band and produced catalogs of sources which were then used for a wide variety of other astrophysical investigations. These surveys were primarily limited by effective area and source confusion at the faintest achievable fluxes. Unlike these previous missions, *Chandra* (Weisskopf et al. 2000) provides arcsecond resolution over a majority of the detector, in particular the Advanced CCD Imaging Spectrometer (ACIS–I, Garmire et al. 1992; Bautz et al. 1998). Superior spatial resolution coupled with a substantial gain in light–gathering power over ROSAT has allowed our 942 ks exposure (hereafter 1Msec) of the CDFS (and the analogous exposure of the Hubble Deep Field North) to become the deepest X–ray exposure(s) ever taken, improving by factors of $\sim$ 20 and $\sim$ 200 the deepest ROSAT and ASCA surveys, respectively.

Along with the *Chandra* Deep Field North (CDFN) (Hornschemeier et al. 2000, 2001; Brandt et al. 2001a,b), the CDFS provides a unique dataset in which to investigate both statistical and source-by-source properties of active galaxies over a large range of redshift and parameter space. Already, the CDFS has discovered both single interesting objects (Norman

et al. 2001) and statistical correlations (Giacconi et al. 2001; Tozzi et al. 2001, hereafter Paper I and II).

The *Chandra* Deep Field South is centered on α = 03:32:28.0, δ=-27:48:30 (J2000), and was selected as having: (1) low Galactic neutral hydrogen column ($N_H \sim 8 \times 10^{19}$ cm^{-2}); (2) no bright stars ($m_V \leq 14$) within 30′ and (3) field accessibility from the new 8m class telescopes, namely VLT and Gemini-South. Note that recent higher–resolution HI maps (from the Parkes Multi–beam Survey; L. Staveley–Smith, private communication) confirm the HI hole in the CDFS, but do show some sub–structure (on $\sim$ 10 arcminute scale) near the *Chandra* pointings, at the level of $10^{19.5}$ cm^{-2}.

Here we present the catalog of the sources in the CDFS field found in the 1Msec exposure along with fluxes (or upper limits) in R, for their presumed optical counterparts. The first scientific results derived from the 1Msec observation are presented in Rosati et al. 2001 (Paper III).

The Paper is structured as follows: in Section 2 we discuss the data, in Section 3 we discuss extraction for point and extended sources and their photometry; in Section 4 the optical identifications are presented. We conclude with a discussion of this dataset. The common catalog is given in Table 2. In Tables 3, 4 and 5 are listed sources detected only by SExtractor and wavelet techniques, and extended properties respectively.

2. X–ray Data

2.1. Diary of Observations

The final X–ray image used to generate the catalog is a combination of 11 individual *Chandra* ACIS–I pointings summarised in Table 1. The maximum total exposure time is 942 ks, but varies across the detector(s), with a minimum of 25 ksec at the edge of the field where we obtained only single exposures due to rotation of the field–of–view. ACIS consists of ten CCDs, distributed in a 2x2 array (ACIS–I) and a 1x6 array (ACIS–S, see the Chandra Observatory Guide at http://asc.harvard.edu/udocs/docs/docs.html). All four ACIS–I chips and the ACIS–S3 chip were used for the CDFS observations. The telescope aimpoint was centered on the ACIS–I3 chip for each exposure. Effective area and spatial resolution of the telescope vary inversely as off–axis angle. Unfortunately the S3 CCD is far enough off–axis to decrease its effective area by a factor of 0.7 (at 4.5 keV) and its spatial resolution by a factor of 0.1 or less relative to the aimpoint. We have therefore chosen to ignore any data in the S3 CCD for the purpose of this work.

Our first two observations in 1999 (1431–0, 1431–1, see Table 1) were taken with the ACIS–I at -110 C. All other observations were taken at -120 C. The CTI–induced QE loss due to grade redistribution (see Townsley et al. 2001) was mitigated by the ten degree change, especially in the hard band. As an example, the effective area improved by 5% at 4.5 keV. The improvement is higher at larger energies, where, however, the effective area is much smaller. The 7 observations taken in December 2000 were processed by the *Chandra* X–ray Center using the most recent calibration files which were introduced in versions R4CU5UPD11 (and later) of the processing software. Those observations taken in 1999 and the summer of 2000 were also re–processed by the *Chandra* X–ray Center using the new calibration files.

2.2. Processing Standards

CIAO 2.0.1 (see http://asc.harvard.edu/ciao) was used to reduce all of the data sets. While calculating exposure maps, the program *asp_apply_sim* was used to fix the shifts between exposure maps and X–ray images. The data were filtered to include only the standard ASCA event grades 0, 2, 3, 4 and 6. All hot pixels and columns were removed. We also removed the flickering pixels (caused mainly by cosmic rays afterglows), defined as the pixels with more than two contiguous events within 3.3 sec. Time intervals with background rates larger than 3σ over the average global value were removed. Due to the high background, about 8800 sec were removed from the level 2 files; most of them were removed from the first exposure, which contained the only long–lasting high background flare. The final exposure time of 942 ks also reflects corrections for CCD read–out time and time lost due to bad satellite aspect.

There are small shifts (between 20" and 1") between the aimpoints of each exposure. We calculated these relative shifts by registering the brightest sources and combining the eleven observations. The combined data has the same coordinate system as Obs. ID 2406. We extracted three images from the total 1Msec data: a soft image (0.5–2.0 keV), a hard image (2.0–7.0 keV) and the total image (0.5–7.0 keV). The images were binned 2×2, which gives an image scale of $0.982''$/pixel. The hard and total bands were cut at 7 keV since above this energy the effective area of *Chandra* is decreasing, while the instrumental background is rising, giving a very inefficient detection of sky and source photons. Figures 1 and 2 shows the soft and hard images. Exposure maps for the soft and hard bands were calculated for each observation, and then combined using the determined shifts and weighting for the individual exposure times. The soft exposure map is shown in Figure 3. A single ACIS–I pointing covers a field of about 0.08 deg^2. Due to the different roll angles of the individual pointings, the final image covers a total of 0.109 deg^2, decreasing rapidly near the flux limit.

The solid angle as a function of the effective exposure time is shown in Figure 4. The sky coverage (see Figure 5) is defined as the solid angle within which a source with a given X–ray flux can be detected at S/N> 2.1. MARX simulations verify that our model for the sky coverage is accurate within a few percent. The computation of the sky coverage and the simulations are described in Tozzi et al. (2001).

3. Detection Techniques

3.1. Sextractor

To detect sources in the Chandra Deep Field South we ran a modified version of the SExtractor algorithm (Bertin & Arnouts 1996) on the 0.5–7 keV image. This modified detection algorithm is several orders of magnitude faster than the wavelet algorithm of Rosati et al. (1995) or WAVDETECT in the CIAO software (Dobrzycki et al. 1999; Freeman et al. 2001). Detection parameters (e.g., threshold, characteristic object size, and ultimately the signal–to–noise) were chosen to find very faint sources, while limiting the number of spurious sources to 10, or approximately $\sim 3\%$ of the total sample. The number of fake sources as a function of the algorithms' parameters was determined via extensive simulations as described in Tozzi et al. (2001).

SExtractor was first run on the 0.5–7 keV image to produce an initial list of candidate sources. SExtractor detection parameters were chosen as a result of simulations and we adopted a detection threshold of 2.4, with a Gaussian filter with 1.5″ FWHM and a minimum area of 5 connected pixels. SExtractor parameters were chosen to detect sources to the faintest limits, thus including a sizeable number of spurious sources. Object photometry for each source was then performed separately in the soft and hard bands and its significance was determined by measuring the signal–to–noise for each source. The definition of S/N was that adopted by Tozzi et al. (2001). Source counts are measured in a circle of radius R_s, where R_s is in units of pixels and is determined by a function $R_s = 2.4'' \times$ FWHM (with a minimum of 5 pixels). The FWHM was modeled as a function of the off–axis angle to reproduce the broadening of the PSF. The parabolic fit we adopted has the coefficients $(a_0, a_1, a_2) = (0.6779, -0.0405, 0.0535)$. The radius R_s reproduces the 95% encircled–energy radius as included in the WAVDETECT algorithm. Note that the fit that we used for photometry is different from the fit of the average FWHM of the observed sources that we used later to select extended sources.

The local background was calculated for each source in an annulus with outer radius of R_s + 12 pixels (11.8″) and inner radius R_s + 2 pixels (1.9″), after masking out nearby

sources. We considered only sources with S/N ≥ 2.1 in either the soft or hard band. This procedure removed 47 sources from the raw catalog obtained with SExtractor. Detailed simulations have shown that a S/N>2.1 threshold results in less than 10 spurious sources in the whole sample. Our simulations have also shown that aperture photometry leads to an underestimate of the source count rate by approximately 4% (see panel c of Figure 1 of Paper II). We have corrected this photometric bias before converting count–rates into energy fluxes. We also notice that our aperture photometry is based on apertures larger than both the hard and soft PSFs, so that we do not suffer any effect from the energy dependent nature of the PSF.

Incidentally, we remark that the same procedure run separately in both the soft and hard bands did not add any new detections. Conversely, the combined catalog obtained from the detections in the two separate bands, was missing several *bona fide* sources found in the 0.5–7 keV image. This is expected since we are far from being background limited: the soft background is $(2.6 \pm 0.4) \times 10^{-7}$ counts/arcsec^2/s, while the hard (2–7 keV) background is $(4.2 \pm 0.5) \times 10^{-7}$ counts/arcsec^2/s. The higher background in the total image is therefore more than compensated for by the higher signal–to–noise of the sources.

We checked the detections by eye, removing a spurious double detection far off–axis, and splitting two blended sources. We checked also that point sources included in the brightest extended sources (see §3.4) are correctly identified. Thus, we have 294 sources with S/N ≥ 2.1 from the soft image, and 247 sources from the hard image. The total number of SExtractor sources is 332. There are 85 only detected in the soft band, and 38 only detected in the hard band.

3.2. Wavelet Transform

To independently check the sources detected with SExtractor, we ran WAVDETECT (Dobrzycki et al. 1999; Freeman et al. 2001) on the 0.5–7 keV image. A probability threshold of 1×10^{-6}, and scales of 1, 1.414, 2.0, 2.828, 4.0, 5.656, 8.0 pixels were used for source identification. The combined image of 1 Msec has $\sim 1.4 \times 10^6$ pixels; therefore we expect ~ 1.4 false detections per image for a uniform, static background. However, this is not the case for our data, where the background is not static and varies across the field, especially at the edges, between individual observations.

Instead of defining another completeness criterium for the sources detected with WAVDETECT, and thus a separate catalog, we use this sample as a complement to the SExtractor catalog. Therefore we apply the same S/N>2.1 threshold on the list of candidates obtained

with WAVDETECT, removing 23 of them. Again, the measure of the signal–to–noise ratio for each source candidate has been done independently in both the soft and hard images, using the same extraction regions described in the previous Section. Finally, we have 288 sources with $S/N > 2.1$ from the soft image, and 240 sources from the hard image. The total number of sources is 318. There are 78 detected in the soft band only, and 30 detected in the hard band only.

3.3. Joint Data Set

We compared the two catalogs from SExtractor and WAVDETECT, using a matching radius of $2''$. We found 304 sources were detected by both methods. These jointly detected sources constitute the first section of the catalog, given in Table 2. We also have 28 sources which are detected by SExtractor only, which we list Table 3, and 14 which are detected by WAVDETECT only, which we list in Table 4. In Figs 6 and 7 we compare the photon counts measured with the SExtractor method with the counts measured with WAVDETECT for each detected source. The comparison has been done both in the soft and hard band. We note an excellent agreement between the independent photometric measurements. It should also be noted that all quoted counts in the catalog (Tables 2-4) were determined using the aperture method described in Section 3.1 above. The adopted cut at $S/N>2.1$ corresponds to $\sim 11(13)$ counts for the faintest sources in the soft(hard) band at the aimpoint. The net count rates were obtained by dividing the net counts by the effective exposure time, which includes the effect of vignetting.

The energy fluxes were computed separately in the soft and hard bands. We prefer to quote the energy flux in the 2–10 keV band as extrapolated from the counts in the 2–7 keV bands, in order to make a direct comparison with previous results from the literature. To derive the energy flux from the observed count rate for the soft and hard bands, we have assumed a conversion factor appropriate for the measured average spectrum of all the sources $\Gamma = 1.375 \pm 0.015$ (found for all the 1 Msec sources). After fixing the local absorption to the Galactic value of 8×10^{19} cm^{-2}, we have a conversion factor of $(4.6 \pm 0.1) \times 10^{-12}$ from count rate to erg s^{-1} cm^{-2} in the soft band and $(3.0 \pm 0.3) \times 10^{-11}$ in the hard band. The uncertainties correspond to $\Gamma = 1.4 \pm 0.3$. The error on the fluxes in the table include only the Poissonian error resulting from the source and background counts. With the adopted conversion factors, the minimum fluxes achieved in the soft and hard band are 5.5×10^{-17} erg s^{-1} cm^{-2} and 4.5×10^{-16} erg s^{-1} cm^{-2}, respectively.

3.4. Extended Sources

The CDFS 1Msec source catalog contains a sizeable fraction of sources which are resolved by Chandra. A search for extended sources in the Msec exposure (Paper III) yielded 18 diffuse sources. For relatively rare objects like groups and clusters of galaxies, which are known to contribute up to $\sim 10\%$ of the soft background at 10^{-14} erg s^{-1} cm^{-2} (Rosati et al. 1995), the CDFS probes the very faint end of their X–ray luminosity function. In order to search for extended sources associated with hot halos of galaxies, groups and clusters, we used the soft image and characterized the source extent with the FWHM of the best fit Gaussian profile. A higher S/N cut, $S/N > 3$, is required for a robust determination of the source extent. The likelihood that a source is extended can be estimated as a function of the off–axis angle by comparing the measured FWHM with the local PSF width. The latter was empirically derived with the same profile fitting procedure by using a sample of 346 sources which were drawn from the combination of the CDFS with two additional deep fields in the *Chandra* Archive, MS1137.5+6625 (sequence number 800044, 120 ks) and CL0848.6+4453 (Lynx field, 800103, 190 ks). This control sample was constructed including only sources with $S/N > 3$ and excluding outliers in the extent distribution with a 3σ clipping procedure. The best fit of the PSF FWHM as a function of the off–axis angle is shown in Figure 10 (top panel) as a solid line. The coefficients of the parabolic fit are: $(a_0, a_1, a_2) = (1.152, 0.193, 0.025)$. This fit was subtracted from each data point to obtain the FWHM residuals (Figure 10, bottom panel). We then fitted a Gaussian distribution to these residuals in four different off–axis angle bins (0-3, 3-6, 6-9, 9-12 arcmin) and derived the 3σ upper values whose parabolic fit defines our cut off line for extended sources (dashed line). A catalog of the 18 extended sources selected in this way is given in Table 5. We have visually inspected these sources to make sure that strong variations in the exposure map do not affect source characterization.

This procedure will generally not work well for very extended low surface brightness sources for which a simple Gaussian fit is not appropriate, or which might have been missed by both our standard detection algorithms. To search for very diffuse sources we used a complementary approach. We ran WAVDETECT with a small characteristic scale to preferentially select point–like sources. These objects are removed from the soft image by replacing the source region with a simulated background. We then rebinned the resulting image to a larger pixel size (4 arcsec) and used WAVDETECT to search for significant sources (probability threshold of 1×10^{-6}) with characteristic scales of 1.0, 1.414, 2.0, 2.828, 4.0, 5.656, 8.0 pixels. We remind the reader that running WAVDETECT on the original image with large characteristic scales would produce poor results due to well-known cross talk between the small and large scales in the wavelet analysis. One diffuse source is clearly detected with this method (#645 detected by WAVDETECT only). This is a low surface brightness feature also apparent by visual inspection of the field (Figure 1, lower right).

We have added this source to our extended source catalog. The K–band finding chart (Figure 11) shows an asymmetric distribution of X–ray emission, which is likely associated with an intermediate redshift poor cluster.

Visual inspection and optical colors indicate that some of them are groups or isolated early type galaxies at $z < 1$. In several cases however, the X–ray emission is dominated by a central, hard component which is likely due to low–level nuclear activity. Of all the 18 diffuse sources, one has been identified (#594; see Figure 12) with a poor cluster at $z = 0.72$. The X–ray luminosity is $L_X(0.5-2\mathrm{keV}) = 4\times10^{42}$ erg s^{-1}, and the temperature $kT = 1.2^{+0.6}_{-0.3}$ keV (1 sigma errors). The stacked spectrum of the three brightest extended sources ($F_X = 1-3$ erg s^{-1} cm^{-2} in the soft band) clearly identified as groups, is well fitted by a Raymond-Smith model with $kT = 1.7^{+0.6}_{-0.4}$ keV, assuming metallicity 0.3 solar and redshift equal to the spectroscopic or photometric one. The mean surface brightness of these diffuse sources, computed as the ratio between the flux and a circular area of 2*FWHM radius, is as low as 10^{-16} erg s^{-1} cm^{-2} arcmin^{-2}, i.e. between 10 and 20 times fainter than the faintest extended sources discovered by ROSAT.

4. Optical Identifications

Our primary optical imaging was obtained using the FORS1 camera on the ANTU (UT-1 at VLT) telescope. The R band mosaics from this data cover $13.6' \times 13.6'$ to depths between 26 and 26.7 (Vega magnitudes). This data does not cover the full CDFS area and must be supplemented with other observations. The ESO Imaging Survey (EIS) has covered this field to moderate depths in several bands, of which we present R (< 26.1 Vega) here (Arnouts et al. 2001; Vandame et al. 2001). The EIS data has been obtained using the Wide Field Imager (WFI) on the ESO-MPG 2.2 meter telescope at La Silla.

The *Chandra* data itself has a pointing accuracy of roughly 1 $''$. Identification of optical counterparts then depends on registering the X–ray and optical data to the highest possible accuracy. To do this we required a stable and fixed astrometric frame. We have chosen to tie all image astrometry to the FORS1 frame as described below.

4.1. Positional Accuracy

The registration of the X–ray to optical coordinates was done by first cross-correlating the optical and X–ray source catalogs assuming that any residual offsets were smaller than the search box size ($10''$). After correcting for the bulk offsets, the correlation was re-run

with a smaller box size. These catalogs were then used to generate an input file for the IRAF task CCMAP, which generates an astrometric solution from the correlated image and sky coordinates. We found shifts in (RA_R - RA_X, Dec_R - Dec_X) of (1.1, -0.8) arcseconds from the FORS1 R band to X–ray imaging (see Figures 8 and 9). The measured positional r.m.s. is $\sim 0\farcs5$. We have adopted $1\farcs5$ as our 3σ error box. Due to the strong effect of off–axis angle on the X–ray PSF and centroid, we scaled the error radius δ_r with off–axis angle (θ) and signal–to–noise: $\delta_r = c_0 * (FWHM'(\theta)/(S/N))^{c_1}$, where $c_0 = 0.77$ and $c_1 = 0.68$ and FWHM′ is the same quadratic as above but is re-normalized such that a source at zero off–axis angle would have the $1\farcs5$ 3σ error box. We are likely over–estimating the number of possible counterparts for some sources. The resulting optical counterpart candidates presented in Tables 2, 3 and 4 are sorted by separation from the X–ray centroid (the optical ids are also marked with boxes in Figures 15, 16 and 17).

After applying the shifts and error estimates we find that 85% of the sources have a counterpart within the 3σ error circle. This percentage is 78% when calculated with the shallower WFI R band data.

4.2. Optically Undetected Sources

About 15% of the sources in our sample have no optical counterpart within the assumed error circle down to the limiting R magnitude. Some of those sources might have unusually high f_x/f_R ratios, extending the known parameter space of X–ray sources, see figure 13 (here f_R is the energy flux in the R–band). We have therefore compared the distribution of the f_x/f_R ratios of our X–ray sources without optical counterparts – which we assumed have the limiting R magnitude – with the analogous distribution for our X–ray sources with optical counterparts. As shown in Figure 14, the distribution of the f_x/f_R lower limits of optically undetected sources (dashed line) is consistent with the high f_x/f_R tail of the distribution of optically detected sources (solid line). For a concise discussion of the nature of these sources see §5.

5. Discussion and Conclusions

We briefly summarize the detection criteria adopted in this Paper. There are three basic steps: 1) a detection algorithm (either SExtractor or WAVDETECT) has been run on the full 0.5–7 keV image to generate a list of source candidates; 2) aperture photometry has been performed independently in the 0.5–2 keV image and 2–7 keV image at the position of each

source candidate; 3) all those sources with S/N>2.1 either in the soft or in the hard image are considered as real sources and appear in our catalogs. This procedure may not reach the deepest sensitivity achievable with our observations, however, it is a good compromise achieving low limiting fluxes without introducing numerous fake sources. As assessed by extensive simulations described in Tozzi et al. (2001), the fraction of fake sources to be expected in our sample is less than 10 (or $\sim 3\%$) with this method. The faintest sources in our samples have approximately 10 net counts. Given the exposure time and the adopted conversion factors the limiting fluxes achieved in the 0.5–2 keV and in the 2–10 keV band are 5.5×10^{-17} erg s^{-1} cm^{-2} and 4.5×10^{-16} erg s^{-1} cm^{-2}, respectively.

These limiting fluxes are about 20 and 200 times lower than that previous X–ray missions in the soft and hard bands respectively. The catalog of sources presented in this Paper allows us to investigate the nature of X–ray faint sources with unprecedented sensitivity, together with their optical properties. Most of the sources in our sample fall within the X–ray to optical flux ratio range typical of AGN as determined from the EMSS sources (Stocke et al. 1991). In addition a significant population of X–ray faint/optically bright sources is observed, with $f_x/f_R \leq 0.1$, lower than those typical of AGNs. Most of these sources are detected in the soft band only (circles in Figure 13). This population of sources has been already partially identified as nearby, bright normal galaxies by Tozzi et al. (2001); Hornschemeier et al. (2001); Barger et al. (2001). Only a few sources seem to have f_x/f_R values higher than usual, which may be obscured AGN at very high redshift. This population of optically faint sources ($R > 25$) is consistent with a mix of obscured AGN at $z = 1 - 3$ and evolved, high–z galaxies (see Alexander et al. 2001; Cowie et al. 2001). The nature of these sources will be investigated in greater detail in following papers.

The data presented here constitute (along with the *Chandra* Deep Field North) the deepest X–ray exposure ever taken. As such, it is a unique dataset for current and future research. A proposal to re–observe this field with *Chandra* will await detailed analysis of the current dataset. However, a SIRTF Legacy program will be observing this field with both MIPS and IRAC during their own deep survey. Also, a 500ks observation with XMM has been planned in the CDFS this year. The high XMM throughput, combined with the arcsec *Chandra* resolution, will allow high quality X–ray spectra and secure optical identifications to be obtained for most of the X–ray sources in the CDFS. The intensive optical and infrared coverage is planned to continue and to be vigorously pursued at ESO. Deep VLA radio observations are being analyzed.

We thank Dr. Harvey Tananbaum for making available 500 kiloseconds of Director Discretionary Time which doubled our original guaranteed time on this field, thus permitting us to achieve the quoted sensitivity. We thank the entire *Chandra* Team for the high degree

of support we have received in carrying out our observing program. In particular, we wish to thank Antonella Fruscione for her constant help in the use of the CXC software. Finally, we thank the anonymous referee for a detailed report that considerably improved the presentation of the results. R. Giacconi and C. Norman gratefully acknowledge support under NASA grant NAG-8-1527 and NAG-8-1133.

REFERENCES

Alexander et al. 2001, AJ, in press, astro-ph/0107450

Arnouts, S., et al. 2001, A&A in press, astro-ph/0103071

Barger, A.J., Cowie, L.L., Mushotzky, R.F., Richards, E.A. 2001, AJ, 121, 662

Bautz, M., et al. 1998, in Proc. SPIE Vol. 3444, X–ray Optics, Instruments and Missions, eds. R.B. Hoover & A.B. Walker, 210

Bertin, E., Arnouts, S. 1996, A&A Supplement, 117, 393

Brandt, W. et al., AJ, 2001a, 122, 1

Brandt, W. et al. 2001b, AJin pres, astro-ph/0108404

Cowie et al. (2001), ApJ, 551, L9

Dobrzycki A. et al., 1999, *Chandra* Detect 1.0 User Guide. *Chandra* X–ray Center, Cambridge

Freeman, P.E., Kashyap, V., Rosner, R., & Lamb, D.Q. 2001, ApJ, submitted

Garmire, G.P., et al. 1992, ApJ, 399, 694

Giacconi, R., et al. 1962 Phys. Rev. Lett., 9, 439

Giacconi, R., et al. 1979 ApJ, 234, 1

Giacconi, R., et al. 2001, ApJ, 551, 624 (Paper I)

Giommi, P., Perri, M., Fiore, F. 2000, A&A, 362, 799

Hasinger, G., Burg, R., Giacconi, R., Schmidt, J., Truemper, J., & Zamorani, G. 1998, A&A 329, 482

Hornschemeier, A., et al. 2000, ApJ, 541, 49

Hornschemeier, A., et al. 2001, ApJ, 554, 742

Matilsky, T., Gursky, H., Kellog, E., Tananbaum, H., & Giacconi, R. 1973, ApJ, 181, 753

Norman, C., et al., submitted to ApJ, astro-ph/0103198

Piccinotti, G., Mushotzky, R.F., Boldt, E.A., et al. 1982, ApJ, 253, 485

Rosati, P., della Ceca, R., Burg, R., Norman, C., Giacconi, R. 1995, ApJ, 445, 11

Rosati, P., et al. 2001, ApJ, in press, astro-ph/0110452 (Paper III)

Schmidt, M., et al. 1998, A&A, 329, 495

Stocke, J.T., Morris, S.L., Gioia, I.M., Maccacaro, T., Schild, R., Wolter, A., Fleming, T.A., Henry, P.J. 1991, ApJS, 76, 813

Townsley, L.K., Broos, P.S., Nousek, J.A., Garmire, G. P. 2001, Nucl. Instr. and Meth. in Phys. Res. A, astro-ph/0111031

Tozzi, P., et al. 2001, ApJ, in press, astro-ph/0103014 (Paper II)

Ueda, Y., Takahashi, T., Inoue, H., et al. 1999, ApJ, 518, 656

Vandame, B. et al. 2001, submitted to A&A, astro-ph/01020300

Weisskopf, M. C., Tananbaum, H.D., van Speybroeck, L.P., O'dell, S.L. 2000, Proc. SPIE, 4012, 2

Table 1. *Chandra* observations of CDFS

Obs. ID	Obs. Date	Exposure Time (ks) [a]	Roll Angle	Aim Point	Count Rate[b]
1431-0	1999 Oct 15	24.983	47.28	3 32 29.4 -27 48 21.8	0.980
1431-1	1999 Nov 23	92.807	47.28	3 32 29.4 -27 48 21.8	0.7846
441	2000 May 27	55.727	166.73	3 32 26.8 -27 48 17.4	0.6812
582	2000 Jun 03	129.869	162.93	3 32 26.8 -27 48 16.4	0.6984
2406	2000 Dec 10	29.564	332.18	3 32 28.4 -27 48 39.3	0.668
2405	2000 Dec 11	59.363	331.81	3 32 29.0 -27 48 46.4	0.670
2312	2000 Dec 13	123.212	329.92	3 32 28.4 -27 48 39.8	0.6528
1672	2000 Dec 16	94.564	326.90	3 32 28.9 -27 48 47.5	0.6589
2409	2000 Dec 19	68.719	319.21	3 32 28.2 -27 48 41.8	0.6570
2313	2000 Dec 21	129937	319.21	3 32 28.2 -27 48 41.9	0.65487
2239	2000 Dec 23	130.250	319.21	3 32 28.2 -27 48 41.8	0.674

[a]effective exposure time after cleaning bad aspect interval and high background intervals (about 8800 s are lost due to high background)

[b]Count rates on four ACIS-I CCD (0.5–7 keV)

Table 2. Main Catalog

ID[a]	XID[b]	CXO CDFS[c]	RA (J2000)[d]	Dec (J2000)[e]	Soft Cts.[f]	Hard Cts.[g]	Exp Time[h]	Soft Flux[i]	Error[j]	Hard Flux[k]	Error[l]	HR[m]	Pos. Err.[n]	Sep.[o]	R[p]
1	576	J033144.3-274927	03 31 44.28	-27 49 27.19	27.00 ± 11.5	···	438.4(433.7)	2.29e-16	9.77e-17	<1.35e-15	···	−1.00 ± 0.00	2.44	···	> 26.10 W
2	548	J033144.7-275158	03 31 44.73	-27 51 58.21	88.80 ± 15.3	35.30 ± 17.4	584.7(575.8)	6.35e-16	1.09e-16	1.62e-15	7.96e-16	−0.42 ± 0.21	1.84	···	> 26.10 W
3	591	J033145.0-275139	03 31 44.96	-27 51 39.71	60.20 ± 14.5	···	620.2(611.8)	4.06e-16	9.78e-17	<1.31e-15	···	−1.00 ± 0.00	1.99	···	> 26.10 W
4	209	J033147.3-275314	03 31 47.33	-27 53 14.96	320.70 ± 19.7	159.10 ± 17.8	214.1(210.7)	3.75e-15	2.31e-16	1.19e-14	1.33e-15	−0.33 ± 0.06	1.60	0.49	25.02 ± 0.28 W
5	238	J033148.0-275046	03 31 48.02	-27 50 46.82	315.90 ± 20.5	115.80 ± 17.1	647.3(644.7)	2.10e-15	1.36e-16	4.88e-15	7.21e-16	−0.46 ± 0.06	1.60	0.64	23.27 ± 0.09 W
6	569	J033148.1-274802	03 31 48.12	-27 48 2.84	74.70 ± 11.9	···	575.1(573.8)	5.60e-16	8.92e-17	<1.09e-15	···	−1.00 ± 0.00	1.79	0.29	24.49 ± 0.18 W
7	604	J033148.6-274715	03 31 48.65	-27 47 15.58	···	47.40 ± 11.8	397.6(396.6)	<1.53e-16	···	2.91e-15	7.23e-16	1.00 ± 0.00	1.99	0.73	26.56 ± 0.48 W
8	225	J033149.5-274634	03 31 49.50	-27 46 34.75	97.40 ± 12	51.10 ± 11.5	256.9(256.3)	1.04e-15	1.28e-16	3.45e-15	7.77e-16	−0.31 ± 0.12	1.71	0.56	22.31 ± 0.04 W
9	179	J033149.6-275034	03 31 49.59	-27 50 34.80	54.90 ± 12.4	27.30 ± 14.1	655.3(655.3)	3.61e-16	8.15e-17	1.13e-15	5.85e-16	−0.34 ± 0.25	1.91	···	> 26.10 W
10	219	J033150.5-275153	03 31 50.46	-27 51 53.71	278.30 ± 19	142.20 ± 17.1	719.2(717.8)	1.80e-15	1.23e-16	5.81e-15	6.99e-16	−0.32 ± 0.06	1.60	···	> 26.10 W
11	547	J033150.6-275237	03 31 50.57	-27 52 37.56	22.00 ± 12.1	36.00 ± 15.3	744.6(741.0)	1.38e-16	7.56e-17	1.43e-15	6.06e-16	0.24 ± 0.33	2.61	0.35	25.70 ± 0.35 W
														1.69	24.30 ± 0.15 W
														2.24	24.12 ± 0.18 W
12	554	J033150.7-275302	03 31 50.71	-27 53 2.26	52.50 ± 13.4	···	746.8(742.0)	3.27e-16	8.35e-17	<1.03e-15	···	−1.00 ± 0.00	2.00	1.91	24.23 ± 0.15 W
13	121	J033151.2-275053	03 31 51.17	-27 50 53.59	64.80 ± 12.3	51.70 ± 14.3	755.3(757.2)	4.10e-16	7.79e-17	2.06e-15	5.69e-16	−0.11 ± 0.17	1.83	1.28	22.44 ± 0.05 W
14	562	J033151.5-274554	03 31 51.48	-27 45 54.54	37.40 ± 8.5	···	301.3(301.1)	4.19e-16	9.52e-17	<1.25e-15	···	−1.00 ± 0.00	1.93	1.08	26.03 ± 0.42 W
15	112	J033152.1-275328	03 31 52.07	-27 53 28.18	40.10 ± 12.1	60.00 ± 15.7	716.7(712.0)	2.60e-16	7.86e-17	2.47e-15	6.47e-16	0.20 ± 0.19	2.13	0.48	24.83 ± 0.20 W
16	546	J033152.4-274753	03 31 52.38	-27 47 53.70	63.70 ± 10.8	47.20 ± 11.9	770.4(775.5)	3.95e-16	6.70e-17	1.84e-15	4.63e-16	−0.15 ± 0.15	1.79	0.30	25.12 ± 0.24 W
17	76	J033152.6-275018	03 31 52.56	-27 50 18.24	235.20 ± 17.3	207.80 ± 17.8	759.2(764.3)	1.48e-15	1.09e-16	8.20e-15	7.02e-16	−0.07 ± 0.06	1.60	0.61	24.38 ± 0.17 W
18	208	J033152.6-274643	03 31 52.58	-27 46 43.18	151.10 ± 14.3	67.30 ± 12.8	737.7(741.3)	9.80e-16	9.27e-17	2.74e-15	5.21e-16	−0.39 ± 0.09	1.64	0.50	21.39 ± 0.03 W
19	230	J033153.6-274844	03 31 53.60	-27 48 44.28	60.20 ± 10.4	23.30 ± 10.6	820.0(828.2)	3.51e-16	6.07e-17	8.48e-16	3.86e-16	−0.45 ± 0.20	1.78	0.37	24.21 ± 0.12 W
20	545	J033154.4-274200	03 31 54.42	-27 42 0.47	11.40 ± 5.8	22.10 ± 7.5	35.6(35.4)	4.53e-16	2.31e-16	5.57e-15	1.89e-15	0.32 ± 0.28	2.70	0.90	24.39 ± 0.17 W
21	544	J033154.6-275104	03 31 54.64	-27 51 4.75	33.50 ± 9.6	37.10 ± 12.5	841.5(848.2)	1.90e-16	5.46e-17	1.32e-15	4.44e-16	0.05 ± 0.22	2.01	···	> 26.10 W
22	585	J033155.4-275028	03 31 55.35	-27 50 28.93	19.50 ± 8.1	···	788.7(797.4)	1.18e-16	4.91e-17	<7.68e-16	···	−1.00 ± 0.00	2.27	1.94	23.41 ± 0.10 W
23	75	J033155.4-275448	03 31 55.44	-27 54 48.49	78.00 ± 10.3	139.50 ± 14.1	147.1(145.8)	1.58e-15	2.09e-16	1.80e-14	1.82e-15	0.29 ± 0.08	1.76	0.72	20.67 ± 0.02 W
24	588	J033155.6-275044	03 31 55.62	-27 50 44.41	73.60 ± 10.7	···	779.3(787.8)	4.52e-16	6.57e-17	<7.91e-16	···	−1.00 ± 0.00	1.73	1.14	19.80 ± 0.01 W
25	232	J033155.9-274922	03 31 55.91	-27 49 22.04	25.50 ± 8.4	···	822.1(833.3)	1.48e-16	4.89e-17	<6.79e-16	···	−1.00 ± 0.00	2.09	0.26	23.58 ± 0.12 W
26	543	J033157.0-275102	03 31 56.96	-27 51 2.02	37.90 ± 8.8	53.60 ± 11.5	794.5(804.4)	2.28e-16	5.30e-17	2.01e-15	4.31e-16	0.17 ± 0.15	1.90	0.61	25.48 ± 0.31 W
														1.59	24.40 ± 0.17 W
27	261	J033157.1-275110	03 31 57.11	-27 51 10.87	31.20 ± 9	93.50 ± 13.2	813.2(822.9)	1.84e-16	5.29e-17	3.43e-15	4.84e-16	0.50 ± 0.12	2.00	···	> 26.10 W
28	74	J033157.8-274209	03 31 57.76	-27 42 9.36	74.90 ± 10.7	44.20 ± 10.3	70.9(70.8)	1.49e-15	2.14e-16	5.57e-15	1.30e-15	−0.26 ± 0.13	1.77	1.53	22.06 ± 0.04 W
29	73	J033158.2-274834	03 31 58.16	-27 48 34.99	278.00 ± 17.7	138.00 ± 14	859.6(874.7)	1.55e-15	9.85e-17	4.76e-15	4.83e-16	−0.34 ± 0.05	1.57	0.40	21.98 ± 0.04 W
30	558	J033158.2-274459	03 31 58.21	-27 44 59.96	38.20 ± 9.1	···	790.0(796.9)	2.31e-16	5.51e-17	<7.33e-16	···	−1.00 ± 0.00	1.92	0.64	21.18 ± 0.02 W
31	72	J033158.3-275043	03 31 58.34	-27 50 43.12	352.00 ± 19.7	224.20 ± 17	806.7(819.6)	2.09e-15	1.17e-16	8.25e-15	6.25e-16	−0.23 ± 0.04	1.56	0.27	24.99 ± 0.22 W
32	542	J033158.5-275437	03 31 58.47	-27 54 37.22	40.40 ± 12.2	29.00 ± 13.5	711.9(707.6)	2.64e-16	7.98e-17	1.20e-15	5.60e-16	−0.16 ± 0.27	2.09	···	> 26.10 W
33	607	J033159.7-275020	03 31 59.68	-27 50 20.40	···	42.00 ± 9.6	826.3(841.4)	<7.84e-17	···	1.51e-15	3.44e-16	1.00 ± 0.00	1.85	1.04	23.48 ± 0.09 W
34	541	J033159.7-274949	03 31 59.74	-27 49 49.22	26.50 ± 7.8	31.60 ± 9	829.3(845.4)	1.53e-16	4.50e-17	1.13e-15	3.21e-16	0.08 ± 0.20	1.99	···	> 26.10 W
35	71	J033200.4-274320	03 32 0.44	-27 43 20.14	458.10 ± 22.6	179.00 ± 16.2	630.9(634.0)	3.47e-15	1.71e-16	8.51e-15	7.70e-16	−0.44 ± 0.04	1.56	0.82	22.10 ± 0.04 F
36	556	J033200.5-275229	03 32 0.47	-27 52 29.53	22.20 ± 8	···	815.7(823.6)	1.30e-16	4.69e-17	<7.02e-16	···	−1.00 ± 0.00	2.16	0.67	22.09 ± 0.03 F
37	213	J033200.6-275354	03 32 0.61	-27 53 54.78	100.10 ± 13.2	85.50 ± 14.9	802.6(803.8)	5.80e-16	7.65e-17	3.12e-15	5.44e-16	−0.08 ± 0.11	1.71	0.98	25.65 ± 0.37 F
38	70	J033201.5-274648	03 32 1.48	-27 46 48.18	118.20 ± 12	339.20 ± 19.5	863.9(883.8)	6.54e-16	6.64e-17	1.16e-14	6.65e-16	0.47 ± 0.04	1.63	1.49	23.62 ± 0.12 F
39	69	J033201.5-274138	03 32 1.50	-27 41 38.83	74.40 ± 10.2	43.90 ± 10.3	70.7(70.6)	1.49e-15	2.04e-16	5.55e-15	1.30e-15	−0.26 ± 0.13	1.76	0.98	24.02 ± 0.19 F
40	68	J033201.6-274327	03 32 1.62	-27 43 27.73	438.40 ± 22.2	178.40 ± 16.8	838.3(842.3)	2.50e-15	1.27e-16	6.39e-15	6.01e-16	−0.42 ± 0.04	1.56	0.46	22.83 ± 0.06 F
41	93	J033202.4-275235	03 32 2.38	-27 52 35.36	56.70 ± 10.1	23.20 ± 9.4	822.6(830.8)	3.30e-16	5.87e-17	8.42e-16	3.41e-16	−0.42 ± 0.18	1.78	0.82	23.67 ± 0.10 F
42	67	J033202.5-274601	03 32 2.52	-27 46 1.16	577.90 ± 24.5	245.70 ± 16.8	704.8(719.5)	3.92e-15	1.66e-16	1.03e-14	7.04e-16	−0.41 ± 0.03	1.54	0.38	23.56 ± 0.08 F
43	133	J033202.6-274430	03 32 2.58	-27 44 30.44	29.50 ± 7.9	30.00 ± 8.9	690.3(695.0)	2.04e-16	5.47e-17	1.30e-15	3.86e-16	0.00 ± 0.20	1.96	···	> 26.74 F
44	540	J033202.7-275053	03 32 2.66	-27 50 53.09	20.30 ± 6.6	18.80 ± 7.6	799.9(816.4)	1.21e-16	3.95e-17	6.94e-16	2.81e-16	−0.05 ± 0.26	2.02	0.46	25.37 ± 0.25 F
45	117	J033203.1-274450	03 32 3.11	-27 44 50.86	103.70 ± 11.8	32.40 ± 9.2	809.4(818.5)	6.13e-16	6.97e-17	1.19e-15	3.39e-16	−0.53 ± 0.11	1.65	0.15	25.47 ± 0.27 F
46	66	J033203.7-274604	03 32 3.72	-27 46 4.62	78.50 ± 10	274.50 ± 17.5	707.2(722.8)	5.31e-16	6.76e-17	1.15e-14	7.30e-16	0.55 ± 0.05	1.67	0.40	20.72 ± 0.01 F
47	65	J033204.0-275330	03 32 3.95	-27 53 30.48	206.10 ± 15.9	73.30 ± 12.7	846.3(852.5)	1.16e-15	8.99e-17	2.59e-15	4.49e-16	−0.48 ± 0.07	1.60	···	> 26.26 F
48	539	J033204.1-273726	03 32 4.06	-27 37 26.22	45.10 ± 9.2	18.70 ± 9.5	10.1(9.7)	2.94e-15	6.00e-16	8.05e-15	4.09e-15	−0.40 ± 0.23	2.05	1.07	23.95 ± 0.10 F

Table 2—Continued

ID[a]	XID[b]	CXO CDFS[c]	RA (J2000)[d]	Dec (J2000)[e]	Soft Cts.[f]	Hard Cts.[g]	Exp Time[h]	Soft Flux[i]	Error[j]	Hard Flux[k]	Error[l]	HR[m]	Pos. Err.[n]	Sep.[o]	R[p]
49	244	J033204.3-274025	03 32 4.33	-27 40 25.64	20.90 ± 8.3	···	71.6(70.9)	4.13e-16	1.64e-16	<2.40e-15	···	−1.00 ± 0.00	2.37	2.10	25.29 ± 0.38 F
50	226	J033204.5-274644	03 32 4.55	-27 46 44.08	83.70 ± 10.2	34.70 ± 8.2	843.7(867.7)	4.74e-16	5.78e-17	1.21e-15	2.85e-16	−0.43 ± 0.11	1.65	···	> 26.74 F
51	267	J033205.0-274128	03 32 4.95	-27 41 28.18	···	52.70 ± 11.3	189.9(189.4)	<1.91e-16	···	4.38e-15	9.39e-16	1.00 ± 0.00	1.90	0.50	23.72 ± 0.20 F
52	99	J033205.2-275356	03 32 5.23	-27 53 56.33	301.60 ± 18.8	157.60 ± 15.9	862.3(866.2)	1.67e-15	1.04e-16	5.49e-15	5.53e-16	−0.32 ± 0.05	1.58	1.01	23.16 ± 0.10 F
53	227	J033205.4-274644	03 32 5.41	-27 46 44.80	17.80 ± 6.2	62.40 ± 9.6	821.0(845.7)	1.04e-16	3.61e-17	2.22e-15	3.42e-16	0.55 ± 0.13	2.03	···	> 26.74 F
54	108	J033205.8-274447	03 32 5.85	-27 44 47.36	51.00 ± 8.9	24.20 ± 8.1	829.0(835.7)	2.94e-16	5.13e-17	8.73e-16	2.92e-16	−0.36 ± 0.17	1.75	0.47	25.48 ± 0.28 F
55	211	J033206.0-275451	03 32 5.96	-27 54 51.26	47.70 ± 10.9	···	670.7(668.0)	3.31e-16	7.56e-17	<9.48e-16	···	−1.00 ± 0.00	1.91	1.01	21.10 ± 0.02 F
56	259	J033206.2-274928	03 32 6.20	-27 49 28.81	23.50 ± 6.5	91.70 ± 10.9	878.6(905.5)	1.28e-16	3.54e-17	3.05e-15	3.63e-16	0.58 ± 0.10	1.89	0.56	24.07 ± 0.12 F
57	560	J033206.3-274537	03 32 6.27	-27 45 37.98	22.40 ± 6.6	···	877.4(895.5)	1.22e-16	3.60e-17	<4.63e-16	···	−1.00 ± 0.00	1.95	1.26	21.93 ± 0.03 F
58	251	J033207.2-275229	03 32 7.21	-27 52 29.82	22.40 ± 6.9	24.60 ± 8.6	873.4(886.5)	1.23e-16	3.78e-17	8.37e-16	2.93e-16	0.04 ± 0.23	2.00	1.77	24.49 ± 0.20 F
59	590	J033207.3-275129	03 32 7.26	-27 51 29.81	16.50 ± 6	···	813.5(831.7)	9.70e-17	3.53e-17	<4.94e-16	···	−1.00 ± 0.00	2.08	0.83	25.07 ± 0.28 F
60	581	J033207.5-274943	03 32 7.47	-27 49 43.68	17.60 ± 6	···	886.5(913.6)	9.50e-17	3.24e-17	<4.29e-16	···	−1.00 ± 0.00	2.00	1.32	24.38 ± 0.19 F
61	114	J033207.7-275214	03 32 7.70	-27 52 14.70	87.00 ± 10.6	79.90 ± 10.9	855.2(869.8)	4.87e-16	5.93e-17	2.77e-15	3.78e-16	−0.05 ± 0.09	1.65	0.27	24.52 ± 0.18 F
62	207	J033208.0-273735	03 32 8.00	-27 37 35.94	64.10 ± 9.5	132.20 ± 13.1	7.6(7.3)	5.60e-15	8.30e-16	7.57e-14	7.50e-15	0.36 ± 0.08	1.88	1.63	24.03 ± 0.16 F
63	155	J033208.0-274240	03 32 8.03	-27 42 40.10	26.30 ± 10.1	36.70 ± 10.9	830.8(833.8)	1.51e-16	5.81e-17	1.33e-15	3.94e-16	0.16 ± 0.24	2.20	0.32	22.37 ± 0.05 F
64	64	J033208.1-274658	03 32 8.08	-27 46 58.15	331.50 ± 18.6	168.60 ± 14	826.2(853.7)	1.92e-15	1.08e-16	5.95e-15	4.94e-16	−0.34 ± 0.04	1.55	0.19	24.77 ± 0.16 F
														1.43	24.72 ± 0.16 F
65	89	J033208.3-274153	03 32 8.31	-27 41 53.81	75.30 ± 11.7	29.00 ± 11.5	816.2(817.2)	4.41e-16	6.86e-17	1.07e-15	4.24e-16	−0.44 ± 0.17	1.76	0.86	24.58 ± 0.23 F
66	243	J033208.5-274047	03 32 8.48	-27 40 47.78	35.60 ± 9.2	38.60 ± 11.9	368.7(366.0)	3.52e-16	9.08e-17	2.42e-15	7.46e-16	0.04 ± 0.20	2.02	···	> 25.72 F
67	538	J033208.6-274649	03 32 8.62	-27 46 49.15	16.20 ± 5.4	19.80 ± 6.7	668.8(689.8)	1.05e-16	3.51e-17	7.87e-16	2.66e-16	0.08 ± 0.23	1.98	0.17	19.18 ± 0.01 F
68	63	J033208.7-274735	03 32 8.74	-27 47 35.34	7300.20 ± 85.6	2417.30 ± 49.5	873.5(903.7)	4.00e-14	4.69e-16	8.06e-14	1.65e-15	−0.52 ± 0.01	1.51	0.37	18.50 ± 0.00 F
69	221	J033208.9-274425	03 32 8.95	-27 44 25.48	19.60 ± 6.5	···	863.6(871.4)	1.09e-16	3.60e-17	<5.12e-16	···	−1.00 ± 0.00	2.04	···	> 26.74 F
70	62	J033209.5-274807	03 32 9.53	-27 48 7.70	186.20 ± 14.3	167.50 ± 14.2	888.4(920.1)	1.00e-15	7.70e-17	5.49e-15	4.65e-16	−0.07 ± 0.06	1.57	0.28	20.39 ± 0.01 F
71	594	J033209.8-274249	03 32 9.83	-27 42 49.68	60.40 ± 11.8	···	838.5(843.1)	3.45e-16	6.73e-17	<6.53e-16	···	−1.00 ± 0.00	1.81	0.95	21.52 ± 0.03 F
														1.72	24.96 ± 0.10 F
72	537	J033209.9-275016	03 32 9.94	-27 50 16.15	15.20 ± 5.9	16.30 ± 6.8	883.8(910.5)	8.23e-17	3.19e-17	5.40e-16	2.25e-16	0.02 ± 0.28	2.07	···	> 26.26 F
73	248	J033210.3-275418	03 32 10.26	-27 54 18.50	19.90 ± 7.6	27.10 ± 10.4	840.9(840.8)	1.13e-16	4.32e-17	9.72e-16	3.73e-16	0.15 ± 0.26	2.16	1.63	23.18 ± 0.07 F
74	61	J033210.6-274309	03 32 10.57	-27 43 9.73	826.60 ± 29.4	316.00 ± 19.3	845.1(850.3)	4.68e-15	1.66e-16	1.12e-14	6.84e-16	−0.45 ± 0.03	1.53	···	> 26.74 F
75	536	J033210.9-274235	03 32 10.89	-27 42 35.42	32.20 ± 9.6	19.50 ± 9.7	848.7(853.2)	1.81e-16	5.41e-17	6.89e-16	3.43e-16	−0.25 ± 0.27	2.01	0.70	19.39 ± 0.01 F
76	60	J033211.0-274415	03 32 10.98	-27 44 15.65	972.40 ± 31.5	338.60 ± 19.4	855.1(865.8)	5.44e-15	1.76e-16	1.18e-14	6.76e-16	−0.49 ± 0.03	1.53	0.33	22.51 ± 0.03 F
77	185	J033211.0-274343	03 32 11.03	-27 43 43.32	14.40 ± 6.3	19.00 ± 8	871.4(879.2)	7.90e-17	3.46e-17	6.52e-16	2.74e-16	0.13 ± 0.30	2.24	0.94	21.80 ± 0.06 F
78	80	J033211.0-274857	03 32 11.04	-27 48 57.06	137.00 ± 12.4	44.20 ± 8.9	899.5(931.2)	7.28e-16	6.59e-17	1.43e-15	2.88e-16	−0.52 ± 0.08	1.59	0.55	25.12 ± 0.24 F
														0.91	24.63 ± 0.20 F
79	97	J033211.1-274054	03 32 11.07	-27 40 54.34	278.30 ± 18.9	118.00 ± 16.4	808.0(805.3)	1.65e-15	1.12e-16	4.42e-15	6.14e-16	−0.40 ± 0.07	1.60	0.33	23.56 ± 0.07 F
80	59	J033211.5-275214	03 32 11.47	-27 52 14.92	289.40 ± 17.6	192.80 ± 14.9	837.9(852.0)	1.65e-15	1.00e-16	6.82e-15	5.27e-16	−0.21 ± 0.05	1.56	0.82	26.47 ± 0.34 F
81	535	J033211.5-274650	03 32 11.49	-27 46 50.56	31.40 ± 6.8	31.60 ± 7.3	720.1(739.4)	2.09e-16	4.52e-17	1.29e-15	2.98e-16	−0.01 ± 0.16	1.77	0.25	22.01 ± 0.02 F
82	236	J033211.5-275006	03 32 11.53	-27 50 6.83	38.40 ± 7.6	14.10 ± 6.9	894.5(921.8)	2.05e-16	4.06e-17	4.61e-16	2.26e-16	−0.47 ± 0.21	1.74	0.68	23.85 ± 0.09 F
83	58	J033211.8-274629	03 32 11.85	-27 46 29.14	106.70 ± 11.2	51.20 ± 8.9	801.9(822.5)	6.36e-16	6.68e-17	1.88e-15	3.26e-16	−0.36 ± 0.09	1.61	0.37	26.00 ± 0.37 F
84	534	J033212.2-274530	03 32 12.24	-27 45 30.64	10.50 ± 5.1	21.60 ± 7	898.4(914.7)	5.59e-17	2.71e-17	7.12e-16	2.31e-16	0.34 ± 0.26	2.25	0.63	21.67 ± 0.02 F
85	149	J033212.3-274621	03 32 12.30	-27 46 21.79	18.40 ± 5.9	23.00 ± 7	710.1(725.8)	1.24e-16	3.97e-17	9.55e-16	2.91e-16	0.10 ± 0.22	1.94	0.37	23.05 ± 0.05 F
86	57	J033213.0-275238	03 32 13.04	-27 52 38.14	133.80 ± 12.3	128.60 ± 12.5	797.5(805.3)	8.02e-16	7.38e-17	4.81e-15	4.68e-16	−0.02 ± 0.07	1.60	0.44	24.04 ± 0.09 F
87	156	J033213.3-275530	03 32 13.28	-27 55 30.04	···	105.90 ± 14.1	781.2(769.4)	<9.69e-17	···	4.15e-15	5.53e-16	1.00 ± 0.00	1.70	0.75	22.81 ± 0.05 F
88	56	J033213.3-274241	03 32 13.30	-27 42 41.51	396.20 ± 21.1	493.80 ± 23.6	853.6(860.1)	2.22e-15	1.18e-16	1.73e-14	8.27e-16	0.11 ± 0.04	1.56	0.37	20.18 ± 0.01 F
89	257	J033213.5-274857	03 32 13.49	-27 48 57.17	18.60 ± 6.1	40.40 ± 8.4	918.6(953.2)	9.68e-17	3.18e-17	1.28e-15	2.66e-16	0.35 ± 0.17	1.93	1.28	24.17 ± 0.12 F
														1.71	25.64 ± 0.32 F
90	600	J033213.9-274526	03 32 13.88	-27 45 26.50	···	22.30 ± 7.3	900.8(916.2)	<5.48e-17	···	7.34e-16	2.40e-16	1.00 ± 0.00	1.95	0.39	23.50 ± 0.09 F
91	266	J033214.0-274249	03 32 13.96	-27 42 49.50	···	38.10 ± 10.1	853.6(861.2)	<7.99e-17	···	1.33e-15	3.54e-16	1.00 ± 0.00	1.92	0.56	21.70 ± 0.03 F
92	533	J033214.0-275602	03 32 13.96	-27 56 2.00	36.40 ± 9.4	50.60 ± 12.4	556.4(547.1)	2.70e-16	6.97e-17	2.40e-15	5.89e-16	0.17 ± 0.17	1.98	···	> 26.10 W
93	583	J033214.0-275001	03 32 13.98	-27 50 1.64	28.50 ± 6.8	···	889.3(917.3)	1.53e-16	3.66e-17	<4.41e-16	···	−1.00 ± 0.00	1.79	···	> 26.26 F
94	55	J033214.1-275101	03 32 14.09	-27 51 1.84	123.80 ± 12	212.70 ± 15.7	890.3(915.2)	6.65e-16	6.45e-17	7.01e-15	5.17e-16	0.25 ± 0.06	1.60	0.17	22.53 ± 0.03 F
95	532	J033214.2-274231	03 32 14.18	-27 42 31.43	25.10 ± 8.4	22.60 ± 9.3	832.9(838.6)	1.44e-16	4.82e-17	8.13e-16	3.34e-16	−0.06 ± 0.26	2.07	0.67	24.59 ± 0.21 F

Table 2—Continued

ID[a]	XID[b]	CXO CDFS[c]	RA (J2000)[d]	Dec (J2000)[e]	Soft Cts.[f]	Hard Cts.[g]	Exp Time[h]	Soft Flux[i]	Error[j]	Hard Flux[k]	Error[l]	HR[m]	Pos. Err.[n]	Sep.[o]	R[p]
96	531	J033214.5-275111	03 32 14.50	-27 51 11.92	14.20 ± 6	35.20 ± 8.1	874.6(898.3)	7.76e-17	3.28e-17	1.18e-15	2.72e-16	0.41 ± 0.20	2.08	0.32	23.73 ± 0.07 F
97	54	J033214.7-275422	03 32 14.67	-27 54 22.90	99.50 ± 11.5	86.70 ± 11.8	780.7(776.7)	6.10e-16	7.05e-17	3.37e-15	4.58e-16	−0.07 ± 0.09	1.65	0.48	26.39 ± 0.46 W
														1.34	25.51 ± 0.31 W
98	593	J033214.8-274403	03 32 14.77	-27 44 3.91	15.60 ± 5.7	···	871.0(884.1)	8.57e-17	3.13e-17	<4.60e-16	···	−1.00 ± 0.00	2.08	···	> 26.10 W
99	530	J033214.9-273843	03 32 14.90	-27 38 43.69	35.00 ± 11.2	68.30 ± 13.8	192.4(188.4)	4.56e-16	1.46e-16	5.73e-15	1.16e-15	0.33 ± 0.17	2.22	1.54	23.13 ± 0.09 W
100	82	J033214.9-275104	03 32 14.94	-27 51 4.86	44.50 ± 8.1	44.70 ± 8.9	910.6(935.6)	2.34e-16	4.25e-17	1.44e-15	2.87e-16	−0.01 ± 0.14	1.71	···	> 26.10 W
101	83	J033215.0-274225	03 32 15.02	-27 42 25.06	151.10 ± 13.6	96.00 ± 12.7	816.2(821.4)	8.85e-16	7.97e-17	3.52e-15	4.66e-16	−0.23 ± 0.08	1.62	1.18	25.47 ± 0.27 W
														1.19	22.47 ± 0.06 W
102	53	J033215.1-275128	03 32 15.07	-27 51 28.30	276.20 ± 17.2	107.10 ± 11.8	855.5(875.4)	1.54e-15	9.62e-17	3.69e-15	4.06e-16	−0.45 ± 0.05	1.55	0.27	21.66 ± 0.03 W
103	587	J033215.4-275038	03 32 15.42	-27 50 38.58	12.60 ± 5.6	···	895.7(921.7)	6.73e-17	2.99e-17	<4.46e-16	···	−1.00 ± 0.00	2.12	1.83	21.00 ± 0.01 F
														2.02	22.34 ± 0.08 F
104	595	J033215.8-273954	03 32 15.82	-27 39 54.76	46.10 ± 12.9	···	649.4(644.2)	3.06e-16	8.56e-17	<1.09e-15	···	−1.00 ± 0.00	2.06	0.46	25.71 ± 0.30 F
105	552	J033215.9-275325	03 32 15.86	-27 53 25.91	39.90 ± 7.7	···	848.9(852.1)	2.25e-16	4.34e-17	<4.83e-16	···	−1.00 ± 0.00	1.77	0.57	22.62 ± 0.04 F
106	580	J033216.2-274943	03 32 16.17	-27 49 43.14	14.20 ± 5.8	···	924.6(960.3)	7.34e-17	3.00e-17	<4.32e-16	···	−1.00 ± 0.00	2.04	1.26	21.22 ± 0.02 F
														1.62	21.69 ± 0.02 F
107	551	J033216.2-275646	03 32 16.17	-27 56 46.07	62.50 ± 11.3	···	472.4(462.3)	5.08e-16	9.19e-17	<1.23e-15	···	−1.00 ± 0.00	1.82	1.32	22.46 ± 0.05 W
108	206	J033216.3-273930	03 32 16.28	-27 39 30.82	1566.10 ± 41.2	460.20 ± 25.7	613.7(607.0)	1.10e-14	2.89e-16	2.06e-14	1.15e-15	−0.54 ± 0.02	1.53	0.47	19.81 ± 0.01 F
109	529	J033216.3-275525	03 32 16.32	-27 55 25.97	23.00 ± 8.3	28.40 ± 10.2	796.0(786.8)	1.38e-16	4.99e-17	1.09e-15	3.91e-16	0.11 ± 0.25	2.16	···	> 26.26 F
110	218	J033216.5-275200	03 32 16.51	-27 52 0.37	30.60 ± 6.9	14.30 ± 6.1	685.4(696.8)	2.14e-16	4.81e-17	6.19e-16	2.64e-16	−0.37 ± 0.21	1.79	0.40	25.78 ± 0.32 F
111	564	J033216.8-274639	03 32 16.77	-27 46 39.25	18.50 ± 6.1	···	910.7(925.2)	9.72e-17	3.20e-17	<4.31e-16	···	−1.00 ± 0.00	1.93	···	> 26.74 F
112	173	J033216.8-274327	03 32 16.84	-27 43 27.95	14.80 ± 6	···	875.5(888.5)	8.09e-17	3.28e-17	<4.96e-16	···	−1.00 ± 0.00	2.18	0.68	22.31 ± 0.03 F
113	528	J033217.1-275402	03 32 17.06	-27 54 2.81	15.70 ± 6.6	19.20 ± 7.7	775.0(774.6)	9.69e-17	4.07e-17	7.47e-16	3.00e-16	0.10 ± 0.29	2.18	2.15	23.41 ± 0.10 F
114	575	J033217.2-274922	03 32 17.17	-27 49 22.80	14.90 ± 6.1	···	928.1(965.6)	7.68e-17	3.14e-17	<4.35e-16	···	−1.00 ± 0.00	2.03	0.49	19.70 ± 0.01 F
115	205	J033217.2-274137	03 32 17.20	-27 41 37.14	31.40 ± 8.7	43.50 ± 10.8	826.5(828.2)	1.82e-16	5.03e-17	1.58e-15	3.93e-16	0.16 ± 0.18	1.99	0.54	25.99 ± 0.42 F
116	52	J033217.2-274304	03 32 17.22	-27 43 4.04	729.10 ± 27.4	216.30 ± 16.1	855.4(865.8)	4.08e-15	1.53e-16	7.53e-15	5.61e-16	−0.55 ± 0.03	1.53	0.22	21.04 ± 0.01 F
117	51	J033217.3-275221	03 32 17.26	-27 52 21.94	95.80 ± 10.8	405.30 ± 20.9	875.8(888.1)	5.23e-16	5.90e-17	1.38e-14	7.10e-16	0.61 ± 0.04	1.62	0.33	23.22 ± 0.07 F
118	584	J033217.9-275008	03 32 17.92	-27 50 8.05	19.70 ± 6.4	···	918.5(953.2)	1.03e-16	3.33e-17	<4.38e-16	···	−1.00 ± 0.00	1.90	0.41	20.32 ± 0.01 F
119	566	J033218.1-274719	03 32 18.11	-27 47 19.50	32.50 ± 7	···	619.6(628.4)	2.32e-16	5.01e-17	<5.40e-16	···	−1.00 ± 0.00	1.75	0.29	20.62 ± 0.01 F
120	87	J033218.3-275242	03 32 18.32	-27 52 42.64	51.80 ± 8.5	···	818.9(827.6)	3.03e-16	4.96e-17	<4.89e-16	···	−1.00 ± 0.00	1.70	0.51	23.98 ± 0.09 F
121	153	J033218.4-275056	03 32 18.43	-27 50 56.33	34.10 ± 7.3	137.00 ± 13	865.9(885.6)	1.88e-16	4.03e-17	4.66e-15	4.43e-16	0.59 ± 0.07	1.75	0.34	23.40 ± 0.10 F
122	601	J033218.5-274557	03 32 18.52	-27 45 57.06	···	19.00 ± 7.1	912.4(925.2)	<5.75e-17	···	6.19e-16	2.31e-16	1.00 ± 0.00	1.99	0.34	22.05 ± 0.02 F
123	527	J033218.6-275414	03 32 18.59	-27 54 14.40	35.80 ± 8.5	19.70 ± 8	852.9(852.2)	2.01e-16	4.77e-17	6.97e-16	2.83e-16	−0.29 ± 0.21	1.86	···	> 26.26 F
124	526	J033218.8-274413	03 32 18.82	-27 44 13.02	12.60 ± 5.6	18.60 ± 7	892.7(908.7)	6.75e-17	3.00e-17	6.17e-16	2.32e-16	0.18 ± 0.28	2.19	0.90	22.99 ± 0.06 F
125	263	J033218.9-275136	03 32 18.94	-27 51 36.58	15.70 ± 5.8	30.50 ± 7.6	736.8(748.9)	1.02e-16	3.76e-17	1.23e-15	3.06e-16	0.31 ± 0.20	2.00	0.51	25.33 ± 0.24 F
														1.51	24.68 ± 0.14 F
126	50	J033219.1-274756	03 32 19.07	-27 47 56.36	48.90 ± 8.1	53.80 ± 8.9	766.7(793.3)	3.05e-16	5.05e-17	2.04e-15	3.38e-16	0.03 ± 0.12	1.67	0.30	24.14 ± 0.11 F
127	249	J033219.5-275406	03 32 19.49	-27 54 6.55	27.30 ± 7.7	21.70 ± 7.7	855.8(857.3)	1.53e-16	4.30e-17	7.63e-16	2.71e-16	−0.12 ± 0.22	1.92	1.64	21.72 ± 0.03 F
128	254	J033219.9-274519	03 32 19.87	-27 45 19.73	···	55.90 ± 9.3	902.7(917.8)	<5.73e-17	···	1.84e-15	3.06e-16	1.00 ± 0.00	1.69	1.49	23.87 ± 0.09 F
129	525	J033219.9-274123	03 32 19.88	-27 41 23.57	36.20 ± 9.4	35.90 ± 11.1	843.7(845.5)	2.05e-16	5.33e-17	1.28e-15	3.96e-16	−0.01 ± 0.20	1.95	0.03	19.15 ± 0.00 F
130	610	J033219.9-275159	03 32 19.93	-27 51 59.76	···	16.20 ± 6.7	800.5(811.5)	<6.52e-17	···	6.02e-16	2.49e-16	1.00 ± 0.00	2.07	···	> 26.26 F
131	524	J033220.0-274243	03 32 20.03	-27 42 43.99	28.20 ± 7.3	31.10 ± 8.8	833.8(841.9)	1.62e-16	4.19e-17	1.11e-15	3.15e-16	0.04 ± 0.19	1.90	···	> 25.72 F
132	253	J033220.1-274448	03 32 20.14	-27 44 48.01	15.30 ± 5.9	77.40 ± 10.5	882.7(898.7)	8.29e-17	3.20e-17	2.60e-15	3.52e-16	0.66 ± 0.11	2.04	0.13	24.94 ± 0.17 F
133	523	J033220.4-274229	03 32 20.44	-27 42 29.05	21.70 ± 7.2	18.60 ± 8.5	846.1(852.8)	1.23e-16	4.07e-17	6.58e-16	3.01e-16	−0.08 ± 0.28	2.04	···	> 25.72 F
134	151	J033220.6-274733	03 32 20.55	-27 47 33.43	···	126.70 ± 12.6	860.3(876.1)	<5.94e-17	···	4.36e-15	4.34e-16	1.00 ± 0.00	1.59	0.42	22.52 ± 0.04 F
135	96	J033220.9-275223	03 32 20.89	-27 52 23.88	43.10 ± 7.9	19.30 ± 7	738.9(747.9)	2.70e-16	4.95e-17	7.54e-16	2.73e-16	−0.39 ± 0.17	1.72	1.39	24.99 ± 0.27 F
														1.40	24.85 ± 0.23 F
136	612	J033221.4-274231	03 32 21.45	-27 42 31.54	···	42.50 ± 9.6	841.9(849.2)	<7.46e-17	···	1.51e-15	3.41e-16	1.00 ± 0.00	1.84	0.81	21.88 ± 0.03 F
														1.56	22.57 ± 0.12 F
137	522	J033221.5-275550	03 32 21.50	-27 55 50.99	68.70 ± 10.8	33.40 ± 11.2	834.8(827.9)	3.94e-16	6.19e-17	1.22e-15	4.08e-16	−0.34 ± 0.16	1.74	0.63	24.13 ± 0.11 F
														1.54	24.81 ± 0.17 F
														1.61	24.15 ± 0.16 F

Table 2—Continued

ID[a]	XID[b]	CXO CDFS[c]	RA (J2000)[d]	Dec (J2000)[e]	Soft Cts.[f]	Hard Cts.[g]	Exp Time[h]	Soft Flux[i]	Error[j]	Hard Flux[k]	Error[l]	HR[m]	Pos. Err.[n]	Sep.[o]	R[p]
138	602	J033222.0-274657	03 32 21.99	-27 46 57.29	···	25.70 ± 7.5	931.5(948.4)	<5.67e-17	···	8.17e-16	2.38e-16	1.00 ± 0.00	1.85	1.17	21.55 ± 0.02 F
139	572	J033222.2-274812	03 32 22.24	-27 48 12.38	14.70 ± 5.4	···	701.5(713.6)	1.00e-16	3.68e-17	<5.39e-16	···	−1.00 ± 0.00	1.95	···	> 26.74 F
140	561	J033222.5-274544	03 32 22.50	-27 45 44.60	20.50 ± 6.1	···	909.3(922.0)	1.08e-16	3.21e-17	<4.79e-16	···	−1.00 ± 0.00	1.88	···	> 26.74 F
141	570	J033222.6-274806	03 32 22.57	-27 48 6.01	26.80 ± 6.8	···	807.2(818.3)	1.59e-16	4.03e-17	<4.83e-16	···	−1.00 ± 0.00	1.79	1.18	24.58 ± 0.17 F
142	188	J033222.6-274950	03 32 22.62	-27 49 50.63	···	19.50 ± 7.2	881.9(914.1)	<6.16e-17	···	6.43e-16	2.37e-16	1.00 ± 0.00	1.95	0.24	22.88 ± 0.07 F
143	145	J033222.6-274604	03 32 22.63	-27 46 4.76	60.20 ± 8.8	105.60 ± 11.9	909.5(921.6)	3.17e-16	4.63e-17	3.45e-15	3.89e-16	0.27 ± 0.09	1.65	0.20	24.78 ± 0.17 F
144	549	J033222.7-275804	03 32 22.70	-27 58 4.91	41.90 ± 11.6	···	363.9(355.6)	3.88e-16	1.07e-16	<1.33e-15	···	−1.00 ± 0.00	2.06	1.77	11.44 ± 0.00 W
145	521	J033222.8-275225	03 32 22.83	-27 52 25.25	37.40 ± 7.5	16.20 ± 7	885.6(899.3)	2.02e-16	4.05e-17	5.43e-16	2.35e-16	−0.40 ± 0.20	1.75	0.53	20.10 ± 0.01 F
146	246	J033222.9-273937	03 32 22.94	-27 39 37.55	71.00 ± 13	43.20 ± 14.3	648.9(643.9)	4.72e-16	8.63e-17	1.82e-15	6.03e-16	−0.24 ± 0.18	1.84	0.09	20.73 ± 0.04 F
147	204	J033223.2-274555	03 32 23.23	-27 45 55.30	16.60 ± 6	···	909.0(922.3)	8.73e-17	3.16e-17	<4.71e-16	···	−1.00 ± 0.00	1.98	0.30	23.42 ± 0.07 F
148	241	J033224.3-274258	03 32 24.30	-27 42 58.10	33.60 ± 7.5	15.80 ± 7.1	833.4(842.3)	1.93e-16	4.30e-17	5.66e-16	2.54e-16	−0.36 ± 0.22	1.83	0.56	24.76 ± 0.17 F
149	49	J033224.3-274127	03 32 24.33	-27 41 27.06	294.80 ± 18.5	105.90 ± 13.8	843.0(844.3)	1.67e-15	1.05e-16	3.78e-15	4.93e-16	−0.47 ± 0.06	1.58	0.27	20.99 ± 0.02 F
150	613	J033224.7-274011	03 32 24.66	-27 40 11.57	···	45.10 ± 13	656.4(654.8)	<1.22e-16	···	1.87e-15	5.39e-16	1.00 ± 0.00	2.05	0.59	23.13 ± 0.07 F
151	598	J033224.7-275413	03 32 24.74	-27 54 13.07	···	15.20 ± 6.9	830.5(838.1)	<6.43e-17	···	5.32e-16	2.42e-16	1.00 ± 0.00	2.23	0.76	21.18 ± 0.01 F
152	48	J033224.9-275601	03 32 24.92	-27 56 1.68	146.00 ± 14.1	135.40 ± 15	846.9(841.5)	8.25e-16	7.96e-17	4.85e-15	5.37e-16	−0.03 ± 0.07	1.63	0.93	24.89 ± 0.21 W
153	565	J033224.9-274707	03 32 24.93	-27 47 7.40	11.70 ± 5.6	···	898.5(911.3)	6.06e-17	2.90e-17	<4.36e-16	···	−1.00 ± 0.00	2.10	0.34	20.69 ± 0.01 F
154	606	J033225.0-275009	03 32 25.04	-27 50 9.06	···	33.10 ± 8	758.0(775.7)	<6.33e-17	···	1.25e-15	3.03e-16	1.00 ± 0.00	1.77	0.48	25.26 ± 0.19 F
155	47	J033225.1-274101	03 32 25.08	-27 41 1.90	39.10 ± 11.5	100.30 ± 15.1	831.9(830.0)	2.25e-16	6.61e-17	3.64e-15	5.49e-16	0.44 ± 0.13	2.02	0.66	21.98 ± 0.02 F
156	260	J033225.2-275044	03 32 25.20	-27 50 44.23	13.10 ± 5.4	21.30 ± 7.1	791.1(808.2)	7.92e-17	3.26e-17	7.95e-16	2.65e-16	0.23 ± 0.25	2.02	0.31	23.81 ± 0.09 F
157	46	J033225.3-274219	03 32 25.26	-27 42 19.44	426.80 ± 21.4	119.20 ± 13	865.1(870.6)	2.36e-15	1.18e-16	4.13e-15	4.50e-16	−0.57 ± 0.04	1.55	0.42	23.01 ± 0.05 F
158	150	J033225.3-275451	03 32 25.26	-27 54 51.34	···	64.30 ± 10.8	849.4(851.8)	<7.55e-17	···	2.28e-15	3.82e-16	1.00 ± 0.00	1.73	0.54	23.02 ± 0.04 F
159	45	J033225.8-274306	03 32 25.76	-27 43 6.24	173.70 ± 13.8	128.20 ± 12.6	817.7(827.1)	1.02e-15	8.07e-17	4.67e-15	4.59e-16	−0.16 ± 0.06	1.59	0.24	25.35 ± 0.30 F
160	233	J033225.8-274937	03 32 25.82	-27 49 37.85	11.70 ± 5.3	···	716.9(733.1)	7.81e-17	3.54e-17	<5.42e-16	···	−1.00 ± 0.00	2.06	1.11	20.46 ± 0.01 F
161	589	J033225.9-275121	03 32 25.89	-27 51 21.20	16.00 ± 6	···	910.8(933.9)	8.40e-17	3.15e-17	<4.40e-16	···	−1.00 ± 0.00	1.99	···	> 26.76 F
162	520	J033225.9-273927	03 32 25.92	-27 39 27.65	52.00 ± 12	36.60 ± 14	614.9(609.7)	3.64e-16	8.41e-17	1.63e-15	6.24e-16	−0.17 ± 0.22	1.95	1.36	23.18 ± 0.07 F
163	519	J033225.9-275508	03 32 25.93	-27 55 8.72	29.40 ± 8	27.70 ± 9	859.9(860.8)	1.64e-16	4.45e-17	9.70e-16	3.15e-16	−0.03 ± 0.21	1.94	1.54	23.38 ± 0.06 F
164	81	J033226.0-274515	03 32 26.04	-27 45 15.08	71.00 ± 9.8	27.80 ± 7.9	906.8(920.0)	3.74e-16	5.17e-17	9.11e-16	2.59e-16	−0.44 ± 0.13	1.64	0.24	26.04 ± 0.38 F
165	44	J033226.6-274036	03 32 26.58	-27 40 36.16	1824.60 ± 43.7	416.30 ± 23.3	800.7(796.0)	1.09e-14	2.61e-16	1.58e-14	8.83e-16	−0.63 ± 0.02	1.52	0.32	19.79 ± 0.01 F
166	203	J033226.7-274013	03 32 26.73	-27 40 13.91	365.20 ± 21.3	199.40 ± 18.2	667.8(666.2)	2.36e-15	1.37e-16	8.13e-15	7.42e-16	−0.29 ± 0.05	1.58	0.41	23.53 ± 0.11 F
167	518	J033226.9-274605	03 32 26.85	-27 46 5.05	16.30 ± 6	17.00 ± 7.1	893.0(906.9)	8.73e-17	3.21e-17	5.65e-16	2.36e-16	0.01 ± 0.28	1.97	···	> 26.67 F
168	43	J033226.9-274146	03 32 26.89	-27 41 46.10	97.60 ± 12	110.80 ± 13.5	846.8(848.6)	5.51e-16	6.78e-17	3.94e-15	4.80e-16	0.06 ± 0.09	1.67	0.78	22.61 ± 0.04 F
169	42	J033227.1-274105	03 32 27.08	-27 41 5.53	7566.40 ± 87.5	2245.50 ± 48.5	833.4(831.3)	4.34e-14	5.02e-16	8.14e-14	1.76e-15	−0.54 ± 0.01	1.51	0.38	19.04 ± 0.00 F
170	41	J033227.7-274145	03 32 27.70	-27 41 45.28	76.80 ± 11.2	246.70 ± 17.9	845.3(847.2)	4.35e-16	6.34e-17	8.78e-15	6.37e-16	0.52 ± 0.06	1.71	0.57	22.24 ± 0.03 F
171	224	J033228.8-274621	03 32 28.81	-27 46 21.22	45.00 ± 7.8	···	865.4(876.7)	2.49e-16	4.31e-17	<4.82e-16	···	−1.00 ± 0.00	1.69	0.28	22.03 ± 0.03 F
172	103	J033228.9-274356	03 32 28.90	-27 43 56.24	110.40 ± 11.5	20.40 ± 7.3	828.7(837.0)	6.37e-16	6.64e-17	7.35e-16	2.63e-16	−0.69 ± 0.10	1.61	0.14	18.19 ± 0.00 F
173	40	J033229.1-275731	03 32 29.10	-27 57 31.25	166.10 ± 15.5	79.60 ± 14.9	503.1(494.4)	1.27e-15	1.18e-16	3.90e-15	7.30e-16	−0.34 ± 0.09	1.65	0.14	20.82 ± 0.02 W
174	264	J033229.8-275146	03 32 29.79	-27 51 46.51	11.40 ± 5.4	46.50 ± 8.8	863.8(891.4)	6.31e-17	2.99e-17	1.57e-15	2.98e-16	0.60 ± 0.16	2.14	1.50	23.44 ± 0.05 F
														2.01	24.29 ± 0.12 F
175	599	J033229.9-275329	03 32 29.88	-27 53 29.94	···	16.30 ± 7.1	883.1(900.1)	<5.94e-17	···	5.46e-16	2.38e-16	1.00 ± 0.00	2.15	0.61	26.45 ± 0.36 F
														0.94	25.16 ± 0.18 F
176	95	J033229.9-274425	03 32 29.92	-27 44 25.15	111.00 ± 11.4	20.00 ± 6.8	812.2(818.0)	6.54e-16	6.71e-17	7.37e-16	2.51e-16	−0.70 ± 0.09	1.61	0.55	16.49 ± 0.00 F
177	202	J033229.9-275106	03 32 29.93	-27 51 6.95	57.30 ± 8.6	74.10 ± 10.1	875.7(904.8)	3.13e-16	4.70e-17	2.47e-15	3.37e-16	0.11 ± 0.10	1.66	0.49	23.97 ± 0.13 F
178	39	J033230.1-274530	03 32 30.06	-27 45 30.71	1261.10 ± 35.8	452.50 ± 22.1	862.4(869.1)	6.99e-15	1.99e-16	1.57e-14	7.67e-16	−0.47 ± 0.02	1.52	0.06	21.02 ± 0.01 F
179	116	J033230.1-274405	03 32 30.07	-27 44 5.35	92.70 ± 10.6	26.50 ± 7.5	804.6(811.2)	5.51e-16	6.30e-17	9.85e-16	2.79e-16	−0.56 ± 0.11	1.63	0.26	16.97 ± 0.00 F
180	78	J033230.1-274524	03 32 30.14	-27 45 24.41	304.70 ± 18.1	90.60 ± 11.1	851.2(857.5)	1.71e-15	1.02e-16	3.19e-15	3.90e-16	−0.54 ± 0.05	1.55	0.14	22.44 ± 0.03 F
181	517	J033230.2-28022	03 32 30.24	-28 0 22.36	74.00 ± 12.7	46.20 ± 14.2	83.8(80.2)	1.48e-15	2.54e-16	6.08e-15	1.87e-15	−0.21 ± 0.17	1.90	1.79	21.88 ± 0.04 W
182	38	J033230.3-274505	03 32 30.30	-27 45 5.40	901.50 ± 30.4	256.00 ± 17	840.5(846.1)	5.13e-15	1.73e-16	9.12e-15	6.06e-16	−0.56 ± 0.03	1.52	0.16	21.93 ± 0.04 W
183	516	J033231.4-274727	03 32 31.41	-27 47 27.82	29.00 ± 6.8	17.10 ± 6.9	868.9(876.0)	1.60e-16	3.74e-17	5.89e-16	2.37e-16	−0.26 ± 0.22	1.76	···	> 26.67 F
184	563	J033231.5-274624	03 32 31.54	-27 46 24.60	11.50 ± 5.5	···	886.5(900.7)	6.20e-17	2.97e-17	<4.57e-16	···	−1.00 ± 0.00	2.15	0.74	23.30 ± 0.09 F
185	574	J033231.7-274854	03 32 31.66	-27 48 54.90	14.80 ± 6	···	899.9(918.6)	7.87e-17	3.19e-17	<4.44e-16	···	−1.00 ± 0.00	2.01	0.90	24.33 ± 0.17 F
186	596	J033231.9-275715	03 32 31.91	-27 57 15.08	···	43.60 ± 12.4	615.1(604.1)	<1.33e-16	···	2.05e-15	5.82e-16	1.00 ± 0.00	2.04	0.27	25.22 ± 0.23 W

Table 2—Continued

ID[a]	XID[b]	CXO CDFS[c]	RA (J2000)[d]	Dec (J2000)[e]	Soft Cts.[f]	Hard Cts.[g]	Exp Time[h]	Soft Flux[i]	Error[j]	Hard Flux[k]	Error[l]	HR[m]	Pos. Err.[n]	Sep.[o]	R[p]
187	37	J033232.2-274156	03 32 32.21	-27 41 56.22	89.90 ± 11.5	56.10 ± 10.9	820.7(819.2)	5.24e-16	6.70e-17	2.06e-15	4.01e-16	-0.23 ± 0.11	1.68	0.63	23.39 ± 0.09 F
188	515	J033232.2-274652	03 32 32.24	-27 46 52.36	15.50 ± 5.6	37.60 ± 8.1	879.8(891.8)	8.43e-17	3.04e-17	1.27e-15	2.74e-16	0.41 ± 0.17	1.95	···	> 26.67 F
189	220	J033232.8-275152	03 32 32.82	-27 51 52.38	50.50 ± 8.3	···	911.7(939.6)	2.65e-16	4.35e-17	<4.50e-16	···	-1.00 ± 0.00	1.68	0.48	23.30 ± 0.02 F
190	36	J033233.1-274548	03 32 33.09	-27 45 48.20	185.10 ± 14.3	86.20 ± 11	872.9(881.6)	1.01e-15	7.84e-17	2.95e-15	3.76e-16	-0.37 ± 0.07	1.57	1.52	20.20 ± 0.01 F
191	217	J033233.2-275206	03 32 33.19	-27 52 6.56	24.20 ± 6.5	···	906.8(933.7)	1.28e-16	3.43e-17	<4.47e-16	···	-1.00 ± 0.00	1.84	···	> 26.76 F
192	265	J033233.4-274236	03 32 33.39	-27 42 36.54	30.40 ± 7.6	83.90 ± 11.3	758.3(759.2)	1.92e-16	4.79e-17	3.33e-15	4.49e-16	0.47 ± 0.11	1.89	···	> 26.00 F
193	514	J033233.6-274312	03 32 33.56	-27 43 12.40	27.30 ± 6.8	20.80 ± 7.4	798.0(801.6)	1.64e-16	4.08e-17	7.82e-16	2.78e-16	-0.14 ± 0.21	1.87	1.32	17.03 ± 0.00 F
194	86	J033233.9-274521	03 32 33.93	-27 45 21.06	23.00 ± 6.5	20.90 ± 7.3	900.3(905.1)	1.22e-16	3.45e-17	6.96e-16	2.43e-16	-0.05 ± 0.22	1.86	0.47	24.65 ± 0.17 F
														1.86	24.62 ± 0.17 F
195	513	J033234.1-274900	03 32 34.07	-27 49 0.55	15.10 ± 5.9	25.10 ± 7.6	852.4(879.7)	8.47e-17	3.31e-17	8.60e-16	2.60e-16	0.23 ± 0.23	1.99	1.97	26.02 ± 0.30 F
196	579	J033234.2-274939	03 32 34.18	-27 49 39.04	22.60 ± 6.4	···	910.4(938.0)	1.19e-16	3.36e-17	<4.09e-16	···	-1.00 ± 0.00	1.83	0.83	24.93 ± 0.14 F
														1.51	25.29 ± 0.19 F
197	183	J033234.2-275641	03 32 34.21	-27 56 41.28	···	42.00 ± 12.4	825.3(819.6)	<1.06e-16	···	1.55e-15	4.56e-16	1.00 ± 0.00	2.04	···	> 26.10 W
198	35	J033234.4-273914	03 32 34.42	-27 39 14.58	93.10 ± 10.7	79.60 ± 10.6	68.8(68.1)	3.72e-15	4.27e-16	2.02e-14	2.70e-15	-0.07 ± 0.09	1.72	1.43	24.32 ± 0.11 F
199	512	J033234.5-274351	03 32 34.45	-27 43 51.13	32.10 ± 7.2	24.40 ± 7.3	857.9(862.2)	1.79e-16	4.01e-17	8.53e-16	2.55e-16	-0.14 ± 0.18	1.81	0.61	22.07 ± 0.04 F
200	247	J033234.9-275535	03 32 34.92	-27 55 35.11	20.80 ± 8.2	40.00 ± 10.3	823.0(828.0)	1.21e-16	4.77e-17	1.46e-15	3.75e-16	0.31 ± 0.21	2.20	···	> 26.76 F
201	34	J033235.0-275512	03 32 35.04	-27 55 12.50	233.30 ± 16.4	122.10 ± 13.4	842.2(850.7)	1.32e-15	9.31e-17	4.33e-15	4.75e-16	-0.32 ± 0.06	1.58	0.52	22.86 ± 0.02 F
202	171	J033235.2-274411	03 32 35.19	-27 44 11.62	23.30 ± 6.5	23.90 ± 7.5	888.4(894.0)	1.25e-16	3.50e-17	8.06e-16	2.53e-16	0.01 ± 0.21	1.88	0.50	23.55 ± 0.06 F
203	148	J033235.3-275319	03 32 35.31	-27 53 19.03	69.40 ± 9.4	70.50 ± 10	885.5(907.2)	3.75e-16	5.08e-17	2.34e-15	3.32e-16	0.00 ± 0.10	1.66	0.31	27.32 ± 0.51 F
204	190	J033236.0-274100	03 32 36.00	-27 41 0.35	···	87.90 ± 14	785.5(778.7)	<1.01e-16	···	3.40e-15	5.42e-16	1.00 ± 0.00	1.75	0.93	22.39 ± 0.02 F
205	100	J033236.0-274851	03 32 36.04	-27 48 51.19	33.60 ± 7.1	···	865.5(891.0)	1.86e-16	3.92e-17	<4.56e-16	···	-1.00 ± 0.00	1.73	0.18	22.00 ± 0.02 F
206	609	J033236.2-275037	03 32 36.24	-27 50 37.86	···	24.10 ± 6.8	758.3(780.1)	<6.87e-17	···	9.31e-16	2.63e-16	1.00 ± 0.00	1.84	0.53	24.98 ± 0.10 F
207	239	J033236.2-275127	03 32 36.25	-27 51 27.72	27.40 ± 6.8	16.30 ± 6.9	907.3(936.7)	1.44e-16	3.58e-17	5.25e-16	2.22e-16	-0.27 ± 0.23	1.80	0.39	24.57 ± 0.10 F
208	577	J033236.3-274933	03 32 36.29	-27 49 33.02	27.80 ± 6.8	···	888.5(915.8)	1.50e-16	3.66e-17	<4.41e-16	···	-1.00 ± 0.00	1.78	0.67	20.99 ± 0.01 F
209	511	J033236.6-274631	03 32 36.63	-27 46 31.30	21.70 ± 6.6	13.40 ± 6.5	817.8(822.2)	1.27e-16	3.86e-17	4.91e-16	2.38e-16	-0.24 ± 0.27	1.87	1.47	21.71 ± 0.02 F
														1.75	23.24 ± 0.06 F
210	33	J033236.8-274407	03 32 36.79	-27 44 7.15	683.70 ± 26.5	294.30 ± 18.1	880.7(885.4)	3.71e-15	1.44e-16	1.00e-14	6.16e-16	-0.40 ± 0.03	1.53	0.33	22.52 ± 0.03 F
211	32	J033237.5-274001	03 32 37.51	-27 40 1.16	136.20 ± 13.5	46.00 ± 10.7	189.6(188.0)	1.97e-15	1.96e-16	4.24e-15	9.86e-16	-0.49 ± 0.10	1.66	0.49	22.36 ± 0.03 F
212	31	J033237.9-275213	03 32 37.85	-27 52 13.44	1000.20 ± 32	325.80 ± 18.9	899.3(925.5)	5.32e-15	1.70e-16	1.06e-14	6.16e-16	-0.52 ± 0.03	1.52	0.24	24.57 ± 0.07 F
213	555	J033238.0-275309	03 32 38.04	-27 53 9.17	11.80 ± 5.2	···	858.3(880.7)	6.57e-17	2.90e-17	<4.49e-16	···	-1.00 ± 0.00	2.19	0.43	25.41 ± 0.13 F
214	79	J033238.1-274627	03 32 38.11	-27 46 27.05	119.10 ± 11.6	49.00 ± 8.6	706.5(713.1)	8.06e-16	7.85e-17	2.07e-15	3.64e-16	-0.42 ± 0.08	1.59	···	> 26.67 F
215	557	J033238.1-274401	03 32 38.13	-27 44 1.07	13.70 ± 5.7	···	860.7(862.8)	7.61e-17	3.17e-17	<4.74e-16	···	-1.00 ± 0.00	2.13	2.06	25.44 ± 0.18 F
216	30	J033238.2-273946	03 32 38.21	-27 39 46.01	356.80 ± 19.6	109.00 ± 11.9	56.6(55.7)	1.31e-14	7.21e-16	2.57e-14	2.81e-15	-0.53 ± 0.04	1.58	0.33	20.42 ± 0.01 F
217	210	J033238.4-275554	03 32 38.42	-27 55 54.52	63.90 ± 10.6	24.30 ± 10.5	832.6(835.3)	3.67e-16	6.09e-17	8.77e-16	3.79e-16	-0.45 ± 0.18	1.77	···	> 26.76 F
218	510	J033238.8-275122	03 32 38.84	-27 51 22.43	13.60 ± 5.2	25.00 ± 6.9	702.9(722.3)	9.25e-17	3.54e-17	1.04e-15	2.88e-16	0.28 ± 0.21	2.01	0.27	25.42 ± 0.22 F
219	582	J033238.9-274957	03 32 38.87	-27 49 57.40	15.10 ± 5.5	···	862.1(886.7)	8.38e-17	3.05e-17	<4.66e-16	···	-1.00 ± 0.00	1.97	0.77	20.21 ± 0.01 F
														1.54	24.71 ± 0.04 F
220	567	J033238.9-274732	03 32 38.87	-27 47 32.96	16.50 ± 6.2	···	909.9(934.2)	8.67e-17	3.26e-17	<4.58e-16	···	-1.00 ± 0.00	1.99	0.24	20.98 ± 0.01 F
221	29	J033239.0-275701	03 32 39.03	-27 57 1.84	329.60 ± 20.3	751.00 ± 30.1	801.2(794.3)	1.97e-15	1.21e-16	2.85e-14	1.14e-15	0.39 ± 0.03	1.59	0.58	18.74 ± 0.01 W
222	201	J033239.1-274440	03 32 39.14	-27 44 40.13	69.70 ± 9.5	61.40 ± 9.7	853.5(855.7)	3.91e-16	5.32e-17	2.16e-15	3.42e-16	-0.06 ± 0.10	1.66	···	> 26.10 W
223	28	J033239.2-274602	03 32 39.16	-27 46 2.57	112.90 ± 11.5	75.50 ± 10.2	760.1(762.8)	7.10e-16	7.24e-17	2.98e-15	4.03e-16	-0.20 ± 0.08	1.60	0.34	20.85 ± 0.01 F
224	605	J033239.2-274833	03 32 39.23	-27 48 33.55	···	15.80 ± 6.8	813.4(838.9)	<6.54e-17	···	5.68e-16	2.44e-16	1.00 ± 0.00	2.05	···	> 26.10 W
225	586	J033239.5-275032	03 32 39.54	-27 50 32.68	14.00 ± 5.4	···	768.7(787.8)	8.48e-17	3.27e-17	<4.69e-16	···	-1.00 ± 0.00	2.02	0.35	22.23 ± 0.01 F
226	27	J033239.8-274851	03 32 39.75	-27 48 51.48	124.50 ± 12.1	177.10 ± 14.5	880.7(905.2)	6.76e-16	6.57e-17	5.90e-15	4.83e-16	0.16 ± 0.06	1.59	0.07	24.54 ± 0.16 F
227	26	J033239.8-274612	03 32 39.80	-27 46 12.00	112.70 ± 11.5	70.90 ± 10	733.1(740.9)	7.35e-16	7.50e-17	2.89e-15	4.07e-16	-0.23 ± 0.08	1.60	0.10	24.55 ± 0.19 F
228	25	J033240.9-275548	03 32 40.93	-27 55 48.36	93.70 ± 12.1	194.80 ± 16.8	823.5(827.3)	5.44e-16	7.03e-17	7.10e-15	6.12e-16	0.35 ± 0.07	1.70	0.90	24.64 ± 0.16 F
229	611	J033241.7-274328	03 32 41.74	-27 43 28.24	···	26.30 ± 8.2	821.8(816.8)	<6.87e-17	···	9.71e-16	3.03e-16	1.00 ± 0.00	2.00	1.25	23.29 ± 0.07 F
														1.63	23.67 ± 0.06 F
														1.85	25.09 ± 0.23 F
230	24	J033242.0-275203	03 32 41.95	-27 52 3.65	210.50 ± 15	100.50 ± 11.1	681.4(698.4)	1.48e-15	1.05e-16	4.34e-15	4.79e-16	-0.36 ± 0.06	1.57	0.35	22.58 ± 0.02 F
231	23	J033242.0-274400	03 32 41.96	-27 44 0.71	224.30 ± 15.6	83.10 ± 10.6	766.6(763.3)	1.40e-15	9.73e-17	3.28e-15	4.19e-16	-0.46 ± 0.06	1.57	0.34	24.93 ± 0.16 F

Table 2—Continued

ID[a]	XID[b]	CXO CDFS[c]	RA (J2000)[d]	Dec (J2000)[e]	Soft Cts.[f]	Hard Cts.[g]	Exp Time[h]	Soft Flux[i]	Error[j]	Hard Flux[k]	Error[l]	HR[m]	Pos. Err.[n]	Sep.[o]	R[p]
232	90	J033242.1-275704	03 32 42.12	-27 57 4.07	463.70 ± 23.6	31.80 ± 13.9	805.4(797.8)	2.75e-15	1.40e-16	1.20e-15	5.25e-16	-0.87 ± 0.05	1.57	0.73	13.82 ± 0.00 W
233	509	J033242.3-275754	03 32 42.29	-27 57 54.83	40.00 ± 11.5	34.50 ± 13.8	554.0(546.9)	3.25e-16	9.34e-17	1.79e-15	7.16e-16	-0.07 ± 0.24	2.11	···	> 26.10 W
234	91	J033242.9-274703	03 32 42.91	-27 47 3.08	108.90 ± 11.5	59.50 ± 9.6	889.5(913.3)	5.86e-16	6.18e-17	1.96e-15	3.17e-16	-0.31 ± 0.09	1.60	0.44	24.10 ± 0.10 F
235	256	J033243.1-274845	03 32 43.12	-27 48 45.79	14.40 ± 5.3	54.00 ± 9.1	813.9(837.8)	8.46e-17	3.11e-17	1.94e-15	3.27e-16	0.57 ± 0.14	1.98	0.37	24.36 ± 0.16 F
236	22	J033243.3-274915	03 32 43.32	-27 49 15.06	607.50 ± 25	201.40 ± 15.2	856.6(880.3)	3.39e-15	1.40e-16	6.90e-15	5.21e-16	-0.51 ± 0.03	1.53	0.09	22.52 ± 0.05 W
237	132	J033244.1-275456	03 32 44.09	-27 54 56.12	40.70 ± 8.9	37.20 ± 10.2	850.7(859.4)	2.29e-16	5.00e-17	1.31e-15	3.58e-16	-0.05 ± 0.17	1.86	1.30	24.89 ± 0.11 F
238	94	J033244.1-274636	03 32 44.11	-27 46 36.16	87.50 ± 10.4	···	866.6(885.6)	4.83e-16	5.74e-17	<4.57e-16	···	-1.00 ± 0.00	1.63	0.71	23.45 ± 0.07 F
239	98	J033244.3-275142	03 32 44.30	-27 51 42.41	75.90 ± 9.7	···	822.0(843.3)	4.42e-16	5.64e-17	<4.72e-16	···	-1.00 ± 0.00	1.65	0.73	19.75 ± 0.00 F
240	21	J033244.4-275252	03 32 44.39	-27 52 52.61	86.10 ± 10.1	23.60 ± 7.4	842.3(861.6)	4.89e-16	5.74e-17	8.26e-16	2.59e-16	-0.58 ± 0.11	1.64	0.43	23.96 ± 0.04 F
241	573	J033244.5-274819	03 32 44.51	-27 48 19.80	12.90 ± 5.6	···	895.4(922.8)	6.89e-17	2.99e-17	<4.27e-16	···	-1.00 ± 0.00	2.09	0.05	20.59 ± 0.02 W
242	20	J033244.5-274941	03 32 44.54	-27 49 41.05	95.40 ± 10.6	124.10 ± 12.4	860.7(883.6)	5.30e-16	5.89e-17	4.23e-15	4.23e-16	0.12 ± 0.07	1.61	0.20	23.71 ± 0.10 W
243	85	J033244.7-274836	03 32 44.68	-27 48 36.61	81.00 ± 10	36.70 ± 8.3	870.3(896.9)	4.45e-16	5.50e-17	1.23e-15	2.79e-16	-0.39 ± 0.11	1.63	0.16	24.78 ± 0.14 F
244	189	J033245.9-274213	03 32 45.88	-27 42 13.82	···	38.90 ± 11.7	779.7(766.7)	<1.10e-16	···	1.53e-15	4.60e-16	1.00 ± 0.00	2.02	0.66	21.25 ± 0.03 F
245	147	J033246.4-274632	03 32 46.43	-27 46 32.70	26.00 ± 6.6	124.20 ± 12.4	800.6(817.7)	1.55e-16	3.94e-17	4.58e-15	4.57e-16	0.65 ± 0.08	1.84	0.38	25.14 ± 0.22 F
246	170	J033246.5-275414	03 32 46.51	-27 54 14.62	34.70 ± 8.3	24.90 ± 9.2	850.6(862.1)	1.95e-16	4.67e-17	8.71e-16	3.22e-16	-0.17 ± 0.21	1.89	0.41	20.69 ± 0.01 F
247	84	J033246.9-274212	03 32 46.87	-27 42 12.85	146.90 ± 14.9	27.60 ± 11.7	763.3(750.2)	9.20e-16	9.34e-17	1.11e-15	4.70e-16	-0.68 ± 0.12	1.64	0.51	16.03 ± 0.00 F
248	252	J033247.1-274346	03 32 47.10	-27 43 46.60	16.50 ± 7	51.90 ± 10.4	834.8(825.1)	9.45e-17	4.01e-17	1.90e-15	3.80e-16	0.52 ± 0.17	2.21	0.67	23.29 ± 0.08 W
249	146	J033247.2-275335	03 32 47.16	-27 53 35.12	71.90 ± 10.3	71.70 ± 11	847.0(861.8)	4.06e-16	5.82e-17	2.51e-15	3.85e-16	-0.01 ± 0.10	1.70	···	> 26.76 F
250	592	J033247.3-275147	03 32 47.28	-27 51 47.84	13.60 ± 5.2	···	763.7(781.5)	8.52e-17	3.26e-17	<4.73e-16	···	-1.00 ± 0.00	2.08	0.68	23.54 ± 0.03 F
251	18	J033248.0-274233	03 32 47.98	-27 42 33.30	1220.80 ± 35.9	779.90 ± 29.8	806.1(793.1)	7.24e-15	2.13e-16	2.97e-14	1.13e-15	-0.21 ± 0.02	1.53	0.46	21.34 ± 0.03 W
252	19	J033248.0-274148	03 32 47.99	-27 41 48.34	552.00 ± 24.3	201.30 ± 16.2	355.4(350.0)	7.43e-15	3.27e-16	1.73e-14	1.40e-15	-0.46 ± 0.04	1.55	0.44	21.73 ± 0.03 W
253	184	J033248.3-275257	03 32 48.30	-27 52 57.18	18.60 ± 6.6	42.80 ± 9.2	766.2(779.0)	1.16e-16	4.12e-17	1.66e-15	3.56e-16	0.39 ± 0.17	2.09	0.69	20.97 ± 0.01 F
254	578	J033248.6-274934	03 32 48.59	-27 49 34.68	15.60 ± 5.6	···	839.4(862.0)	8.89e-17	3.19e-17	<4.58e-16	···	-1.00 ± 0.00	2.03	0.89	24.43 ± 0.13 F
														1.59	27.50 ± 0.45 F
255	17	J033249.3-275505	03 32 49.27	-27 55 5.59	119.30 ± 13.4	49.80 ± 12.3	835.3(839.6)	6.83e-16	7.67e-17	1.79e-15	4.42e-16	-0.41 ± 0.11	1.67	0.37	24.59 ± 0.14 F
256	268	J033249.3-274050	03 32 49.34	-27 40 50.20	···	28.20 ± 9	62.6(62.2)	<2.65e-16	···	4.41e-15	1.41e-15	1.00 ± 0.00	2.17	1.28	24.58 ± 0.15 F
														1.32	22.33 ± 0.03 F
257	92	J033249.8-275455	03 32 49.77	-27 54 55.30	213.80 ± 16.4	37.00 ± 11.4	835.3(840.2)	1.22e-15	9.39e-17	1.33e-15	4.09e-16	-0.71 ± 0.08	1.60	0.85	16.91 ± 0.00 F
258	138	J033250.1-274135	03 32 50.11	-27 41 35.30	51.80 ± 9.1	···	87.8(86.6)	9.11e-16	1.60e-16	<1.78e-15	···	-1.00 ± 0.00	1.82	1.04	22.14 ± 0.04 W
														1.29	22.74 ± 0.05 W
259	159	J033250.4-275253	03 32 50.36	-27 52 53.00	396.40 ± 20.6	218.90 ± 16.4	854.3(867.0)	2.22e-15	1.15e-16	7.61e-15	5.70e-16	-0.30 ± 0.04	1.55	···	> 26.76 F
260	597	J033251.4-275544	03 32 51.38	-27 55 44.44	···	25.10 ± 13.1	815.9(814.4)	<1.03e-16	···	9.29e-16	4.85e-16	1.00 ± 0.00	2.54	0.67	24.69 ± 0.10 F
261	508	J033251.8-275214	03 32 51.78	-27 52 14.34	14.20 ± 6.2	28.40 ± 7.9	702.4(712.8)	9.67e-17	4.22e-17	1.20e-15	3.34e-16	0.33 ± 0.23	2.24	···	> 26.76 F
262	242	J033251.9-274229	03 32 51.93	-27 42 29.84	36.90 ± 8.9	···	429.7(425.8)	4.11e-16	9.91e-17	<1.31e-15	···	-1.00 ± 0.00	1.94	0.55	22.49 ± 0.03 F
263	175	J033252.0-274437	03 32 51.95	-27 44 37.61	22.30 ± 7.8	···	824.6(832.2)	1.29e-16	4.52e-17	<6.33e-16	···	-1.00 ± 0.00	2.09	0.54	20.27 ± 0.01 F
264	186	J033252.4-274557	03 32 52.39	-27 45 57.89	15.80 ± 6.2	···	837.6(852.2)	9.02e-17	3.54e-17	<5.20e-16	···	-1.00 ± 0.00	2.15	0.50	23.09 ± 0.06 F
265	15	J033253.0-275120	03 32 52.98	-27 51 20.77	451.60 ± 21.8	175.00 ± 14.5	837.0(849.6)	2.58e-15	1.25e-16	6.21e-15	5.15e-16	-0.45 ± 0.04	1.55	0.28	22.62 ± 0.02 F
266	222	J033254.6-274501	03 32 54.59	-27 45 1.94	128.50 ± 13.1	55.40 ± 11	815.6(825.0)	7.54e-16	7.68e-17	2.02e-15	4.02e-16	-0.40 ± 0.09	1.64	0.68	23.76 ± 0.10 W
267	200	J033255.0-274506	03 32 55.03	-27 45 6.84	111.00 ± 12.6	84.50 ± 12.2	819.4(828.6)	6.48e-16	7.35e-17	3.07e-15	4.44e-16	-0.14 ± 0.09	1.65	0.84	23.53 ± 0.11 F
														1.41	25.64 ± 0.32 F
268	101	J033255.6-274752	03 32 55.60	-27 47 52.22	107.50 ± 11.4	43.30 ± 9.3	850.8(867.2)	6.04e-16	6.41e-17	1.51e-15	3.23e-16	-0.43 ± 0.10	1.63	0.43	24.69 ± 0.12 F
269	229	J033256.5-274835	03 32 56.47	-27 48 35.03	37.90 ± 7.9	···	775.0(788.9)	2.34e-16	4.87e-17	<5.64e-16	···	-1.00 ± 0.00	1.81	0.77	17.06 ± 0.00 F
270	553	J033256.8-275318	03 32 56.78	-27 53 18.46	32.60 ± 9	···	737.0(740.6)	2.12e-16	5.84e-17	<7.66e-16	···	-1.00 ± 0.00	1.99	1.13	20.02 ± 0.00 F
														1.62	21.52 ± 0.01 F
271	177	J033257.1-275009	03 32 57.06	-27 50 9.17	27.90 ± 7.9	···	832.9(843.2)	1.60e-16	4.54e-17	<6.06e-16	···	-1.00 ± 0.00	1.96	0.45	23.78 ± 0.04 F
														1.45	25.69 ± 0.14 F
														1.90	25.85 ± 0.22 F
272	559	J033257.3-274534	03 32 57.26	-27 45 34.60	32.70 ± 8.9	···	832.5(841.2)	1.88e-16	5.11e-17	<6.53e-16	···	-1.00 ± 0.00	1.95	0.89	17.94 ± 0.00 F
273	122	J033257.7-274549	03 32 57.70	-27 45 49.03	63.30 ± 10.3	41.50 ± 10.8	824.9(833.7)	3.67e-16	5.97e-17	1.50e-15	3.91e-16	-0.21 ± 0.15	1.75	0.50	23.14 ± 0.07 F
274	603	J033257.8-274711	03 32 57.79	-27 47 11.11	···	18.60 ± 8.6	817.2(828.9)	<8.12e-17	···	6.77e-16	3.13e-16	1.00 ± 0.00	2.30	0.46	25.52 ± 0.34 F
														0.87	26.99 ± 0.54 F

Table 2—Continued

ID[a]	XID[b]	CXO CDFS[c]	RA (J2000)[d]	Dec (J2000)[e]	Soft Cts.[f]	Hard Cts.[g]	Exp Time[h]	Soft Flux[i]	Error[j]	Hard Flux[k]	Error[l]	HR[m]	Pos. Err.[n]	Sep.[o]	R[p]
275	237	J033258.6-275008	03 32 58.61	-27 50 8.63	72.90 ± 10.4	···	816.2(824.7)	4.27e-16	6.09e-17	<6.31e-16	···	−1.00 ± 0.00	1.71	0.09	17.80 ± 0.00 F
276	110	J033258.7-274633	03 32 58.71	-27 46 33.53	52.30 ± 9.7	34.50 ± 10.1	816.4(825.9)	3.06e-16	5.68e-17	1.26e-15	3.69e-16	−0.21 ± 0.17	1.79	0.74	23.25 ± 0.08 F
277	13	J033259.1-274340	03 32 59.14	-27 43 40.30	473.70 ± 23.2	175.30 ± 16.3	313.3(312.7)	4.70e-15	2.30e-16	1.10e-14	1.02e-15	−0.46 ± 0.04	1.56	0.49	20.93 ± 0.01 F
														0.64	20.81 ± 0.01 F
278	240	J033259.2-275140	03 32 59.20	-27 51 40.43	43.70 ± 9.3	32.70 ± 10.3	816.1(820.8)	2.56e-16	5.45e-17	1.20e-15	3.78e-16	−0.15 ± 0.19	1.86	1.48	25.00 ± 0.21 F
279	152	J033259.4-274859	03 32 59.43	-27 48 59.58	54.00 ± 9.5	179.40 ± 15.5	772.8(782.7)	3.34e-16	5.88e-17	6.91e-15	5.97e-16	0.53 ± 0.07	1.77	0.36	23.04 ± 0.08 F
280	12	J033259.8-275031	03 32 59.79	-27 50 31.34	414.30 ± 21.4	139.80 ± 14.3	819.5(826.4)	2.42e-15	1.25e-16	5.10e-15	5.22e-16	−0.50 ± 0.04	1.56	0.19	19.89 ± 0.01 F
281	10	J033259.9-274627	03 32 59.89	-27 46 27.01	150.60 ± 14.3	210.70 ± 16.8	797.1(804.7)	9.04e-16	8.58e-17	7.89e-15	6.29e-16	0.16 ± 0.06	1.63	0.94	20.69 ± 0.02 F
282	11	J033260.0-274748	03 32 59.95	-27 47 48.80	1044.90 ± 33.1	341.00 ± 20	771.5(781.0)	6.48e-15	2.05e-16	1.32e-14	7.72e-16	−0.51 ± 0.03	1.53	0.17	21.83 ± 0.02 F
283	507	J033300.1-274925	03 33 0.12	-27 49 25.50	23.70 ± 8.2	29.40 ± 9.5	761.0(769.4)	1.49e-16	5.15e-17	1.15e-15	3.72e-16	0.10 ± 0.23	2.09	1.70	24.41 ± 0.18 W
														2.09	22.80 ± 0.06 W
284	550	J033300.8-275749	03 33 0.80	-27 57 49.00	37.70 ± 8.4	···	7.4(6.8)	2.43e-15	5.41e-16	<6.92e-15	···	−1.00 ± 0.00	2.07	1.80	24.28 ± 0.15 W
285	9	J033300.9-275521	03 33 0.91	-27 55 21.47	99.40 ± 10.6	27.00 ± 7.2	8.0(7.9)	5.89e-15	6.29e-16	1.02e-14	2.72e-15	−0.57 ± 0.10	1.71	0.80	22.18 ± 0.04 W
286	174	J033301.2-274421	03 33 1.24	-27 44 21.55	20.40 ± 9	22.40 ± 10.9	585.9(585.5)	1.67e-16	7.35e-17	1.15e-15	5.61e-16	0.05 ± 0.33	2.38	0.67	25.37 ± 0.25 F
287	8	J033301.5-274142	03 33 1.54	-27 41 42.72	77.20 ± 11.1	65.90 ± 12.5	71.3(70.2)	1.53e-15	2.20e-16	8.37e-15	1.59e-15	−0.07 ± 0.12	1.79	0.37	23.43 ± 0.10 W
288	77	J033301.7-274543	03 33 1.68	-27 45 43.20	196.30 ± 16.2	69.10 ± 13	796.2(799.4)	1.18e-15	9.73e-17	2.61e-15	4.90e-16	−0.48 ± 0.08	1.61	0.65	20.63 ± 0.01 F
289	7	J033301.8-275818	03 33 1.77	-27 58 18.59	146.40 ± 13.3	68.40 ± 12.1	4.5(4.3)	1.53e-14	1.39e-15	4.71e-14	8.33e-15	−0.34 ± 0.09	1.71	0.98	20.26 ± 0.02 W
290	6	J033302.7-274823	03 33 2.73	-27 48 23.47	580.60 ± 25.2	186.00 ± 16.6	779.8(784.5)	3.56e-15	1.55e-16	7.15e-15	6.38e-16	−0.52 ± 0.04	1.55	0.82	23.67 ± 0.14 F
291	506	J033303.1-275147	03 33 3.08	-27 51 47.84	88.60 ± 12.1	29.90 ± 11	520.4(519.4)	6.54e-16	8.93e-17	1.39e-15	5.13e-16	−0.49 ± 0.15	1.72	···	> 26.10 W
292	4	J033303.7-274519	03 33 3.72	-27 45 19.08	474.70 ± 23.8	164.60 ± 18.1	790.1(788.7)	2.87e-15	1.44e-16	6.29e-15	6.92e-16	−0.48 ± 0.05	1.56	0.24	22.80 ± 0.05 F
293	571	J033303.9-274811	03 33 3.85	-27 48 11.20	32.50 ± 10.3	···	791.0(793.7)	1.96e-16	6.23e-17	<8.04e-16	···	−1.00 ± 0.00	2.06	0.24	26.14 ± 0.35 F
294	608	J033304.0-275027	03 33 3.96	-27 50 27.24	···	30.70 ± 10.3	609.4(609.7)	<1.19e-16	···	1.43e-15	4.79e-16	1.00 ± 0.00	2.14	0.34	21.81 ± 0.04 W
295	505	J033305.0-274732	03 33 4.96	-27 47 32.82	18.40 ± 9.6	36.40 ± 12.4	781.1(781.6)	1.13e-16	5.88e-17	1.40e-15	4.78e-16	0.33 ± 0.28	2.53	0.89	25.48 ± 0.23 F
														1.77	24.64 ± 0.15 F
296	504	J033305.8-275215	03 33 5.78	-27 52 15.56	25.20 ± 8.4	35.70 ± 10.5	305.0(302.3)	3.05e-16	1.02e-16	2.75e-15	8.08e-16	0.18 ± 0.22	2.18	0.53	19.50 ± 0.01 W
297	3	J033306.0-274651	03 33 5.99	-27 46 51.38	103.60 ± 13.8	77.70 ± 15	787.7(785.6)	6.29e-16	8.38e-17	2.98e-15	5.76e-16	−0.14 ± 0.12	1.72	···	> 26.00 F
298	503	J033307.7-275127	03 33 7.74	-27 51 27.72	310.00 ± 19.5	129.40 ± 14.8	343.8(340.4)	3.33e-15	2.09e-16	8.84e-15	1.01e-15	−0.41 ± 0.05	1.59	0.42	20.82 ± 0.03 W
299	502	J033308.3-275033	03 33 8.26	-27 50 33.43	30.30 ± 9.8	50.80 ± 12.7	458.0(453.9)	2.54e-16	8.22e-17	2.71e-15	6.77e-16	0.26 ± 0.19	2.16	0.63	21.57 ± 0.04 W
300	2	J033308.9-274255	03 33 8.86	-27 42 55.22	143.10 ± 14	29.80 ± 12.1	70.5(69.0)	2.87e-15	2.81e-16	3.86e-15	1.57e-15	−0.65 ± 0.12	1.70	0.12	22.84 ± 0.06 W
301	176	J033309.3-274449	03 33 9.35	-27 44 49.63	56.70 ± 11.9	31.90 ± 12.5	209.9(206.9)	7.63e-16	1.60e-16	2.74e-15	1.08e-15	−0.27 ± 0.20	1.92	0.96	22.28 ± 0.05 W
302	1	J033309.6-274604	03 33 9.62	-27 46 4.12	137.70 ± 15	93.80 ± 14.7	445.5(440.2)	1.39e-15	1.52e-16	6.04e-15	9.47e-16	−0.18 ± 0.09	1.69	0.49	19.86 ± 0.01 W
303	501	J033310.3-274843	03 33 10.31	-27 48 43.20	582.00 ± 25.8	256.60 ± 19.4	434.6(429.7)	5.14e-15	2.28e-16	1.45e-14	1.09e-15	−0.38 ± 0.04	1.56	0.55	22.93 ± 0.07 W
304	568	J033311.2-274735	03 33 11.16	-27 47 35.23	35.00 ± 11.6	···	383.6(378.5)	3.07e-16	1.02e-16	<1.31e-15	···	−1.00 ± 0.00	2.20	2.05	25.78 ± 0.29 W

[a] Optical cutout ID number, in order of RA

[b] Unique Detection ID

[c] IAU Registered Name, based on original (not offset) X–ray coordinates

[d] Right Ascension, offset from *Chandra* by $-1.2''$

[e] Declination, offset from *Chandra* by $0.8''$

[f] Net Counts in soft (0.5 - 2 keV) band

[g] Net Counts in hard (2 - 10 keV) band

[h] Effective exposure time in the soft(hard) band, in kiloseconds

[i] Flux in soft (0.5 - 2 keV) band, c.g.s. units

[j] Error on soft flux

[k] Flux in hard (2 - 10 keV) band, c.g.s. units

[l] Error on hard flux

[m] Hardness Ratio, defined as (H - S)/(H + S) where H and S are the net counts in the hard and soft bands respectively

[n] Error on the X-ray source position as calculated in the text, in arcseconds

[o] Separation of the candidate optical counterpart, in arcseconds

[p] Vega R magnitude for the optical counterpart in either the FORS (F) or WFI (W) filter

Table 3. SExtractor Only

ID[a]	XID[b]	CXO CDFS[c]	RA (J2000)[d]	Dec (J2000)[e]	Soft Cts.[f]	Hard Cts.[g]	Exp Time[h]	Soft Flux[i]	Error[j]	Hard Flux[k]	Error[l]	HR[m]	Pos. Err.[n]	Sep.[o]	R[p]
1	636	J033150.5-275043	03 31 50.45	-27 50 43.62	···	33.60 ± 13.2	657.5(658.4)	<1.23e-16	···	1.39e-15	5.45e-16	1.00 ± 0.00	2.24	1.08	25.50 ± 0.30 W
2	633	J033150.5-275213	03 31 50.52	-27 52 13.33	···	34.30 ± 14.9	732.0(729.8)	<1.34e-16	···	1.38e-15	5.99e-16	1.00 ± 0.00	2.34	···	> 26.10 W
3	619	J033155.6-275403	03 31 55.62	-27 54 3.49	23.60 ± 11	···	757.9(754.3)	1.45e-16	6.75e-17	<9.97e-16	···	−1.00 ± 0.00	2.48	···	> 26.10 W
4	625	J033200.9-274758	03 32 0.88	-27 47 58.88	14.70 ± 6.2	···	876.2(897.8)	8.02e-17	3.38e-17	<5.10e-16	···	−1.00 ± 0.00	2.20	1.86	21.68 ± 0.02 F
5	615	J033201.3-275052	03 32 1.34	-27 50 52.26	14.80 ± 6.5	17.80 ± 7.8	799.3(814.7)	8.86e-17	3.89e-17	6.59e-16	2.89e-16	0.08 ± 0.31	2.25	0.69	23.41 ± 0.09 F
6	626	J033209.5-274758	03 32 9.47	-27 47 58.92	17.20 ± 6.1	···	877.1(908.1)	9.38e-17	3.33e-17	<4.64e-16	···	−1.00 ± 0.00	2.00	1.58	25.35 ± 0.17 F
7	178	J033213.9-275034	03 32 13.89	-27 50 34.84	15.90 ± 5.9	···	904.3(930.5)	8.41e-17	3.12e-17	<4.29e-16	···	−1.00 ± 0.00	2.00	···	> 26.26 F
8	631	J033215.2-274335	03 32 15.19	-27 43 35.94	19.40 ± 6.3	···	878.8(892.5)	1.06e-16	3.43e-17	<4.84e-16	···	−1.00 ± 0.00	2.01	0.75	24.35 ± 0.20 F
9	621	J033216.6-275247	03 32 16.59	-27 52 47.68	13.80 ± 5.8	···	844.1(851.9)	7.82e-17	3.29e-17	<4.90e-16	···	−1.00 ± 0.00	2.15	1.50	24.70 ± 0.22 F
														1.50	25.15 ± 0.34 F
10	635	J033216.9-275009	03 32 16.93	-27 50 9.92	···	15.70 ± 6.6	901.3(932.8)	<6.15e-17	···	5.07e-16	2.13e-16	1.00 ± 0.00	2.04	1.68	25.36 ± 0.24 F
														1.73	23.01 ± 0.05 F
11	640	J033217.7-273852	03 32 17.74	-27 38 52.08	···	28.00 ± 14.1	483.8(475.7)	<1.69e-16	···	1.55e-15	7.81e-16	1.00 ± 0.00	2.65	···	> 25.72 F
12	627	J033223.5-274852	03 32 23.52	-27 48 52.70	12.20 ± 5.3	···	789.0(822.5)	7.40e-17	3.21e-17	<4.64e-16	···	−1.00 ± 0.00	2.03	1.35	19.84 ± 0.01 F
13	616	J033225.6-275843	03 32 25.58	-27 58 43.18	26.20 ± 12.2	···	280.5(272.8)	3.00e-16	1.40e-16	<1.83e-15	···	−1.00 ± 0.00	2.55	···	> 26.10 W
14	637	J033225.7-274332	03 32 25.74	-27 43 32.41	···	21.80 ± 7.3	855.2(866.0)	<6.13e-17	···	7.59e-16	2.54e-16	1.00 ± 0.00	2.00	···	> 25.72 F
15	630	J033228.3-274404	03 32 28.31	-27 44 4.06	23.20 ± 6.6	···	839.5(847.9)	1.32e-16	3.76e-17	<4.78e-16	···	−1.00 ± 0.00	1.89	0.53	23.05 ± 0.10 F
16	623	J033228.6-274659	03 32 28.56	-27 46 59.66	15.40 ± 5.7	···	885.4(893.5)	8.09e-17	3.00e-17	<4.49e-16	···	−1.00 ± 0.00	1.95	0.52	25.40 ± 0.33 F
														1.67	24.92 ± 0.16 F
17	624	J033229.3-274708	03 32 29.31	-27 47 8.45	15.40 ± 5.8	···	919.7(928.2)	8.01e-17	3.02e-17	<4.63e-16	···	−1.00 ± 0.00	1.97	0.22	21.70 ± 0.02 F
18	618	J033229.4-275620	03 32 29.44	-27 56 20.18	28.40 ± 8.9	···	848.8(844.1)	1.60e-16	5.01e-17	<7.55e-16	···	−1.00 ± 0.00	2.07	0.84	25.57 ± 0.29 W
19	638	J033230.0-274302	03 32 29.98	-27 43 2.78	···	13.90 ± 6.9	865.7(872.3)	<6.19e-17	···	4.80e-16	2.39e-16	1.00 ± 0.00	2.31	0.45	23.60 ± 0.10 F
														0.71	22.76 ± 0.10 F
														0.96	23.89 ± 0.08 F
20	620	J033230.2-275307	03 32 30.25	-27 53 7.55	15.50 ± 5.8	···	899.7(917.9)	8.24e-17	3.08e-17	<4.69e-16	···	−1.00 ± 0.00	2.05	0.82	21.43 ± 0.01 F
														1.16	23.04 ± 0.02 F
21	617	J033231.5-275725	03 32 31.53	-27 57 25.88	34.40 ± 10.8	···	522.6(513.5)	2.53e-16	7.94e-17	<1.05e-15	···	−1.00 ± 0.00	2.10	1.30	21.37 ± 0.03 W
22	632	J033233.5-275228	03 32 33.54	-27 52 28.60	···	17.30 ± 7	889.4(913.2)	<5.83e-17	···	5.71e-16	2.31e-16	1.00 ± 0.00	2.08	1.96	26.97 ± 0.51 F
23	614	J033234.7-274040	03 32 34.70	-27 40 40.26	28.60 ± 9.6	29.40 ± 11.8	755.1(751.4)	1.81e-16	6.08e-17	1.18e-15	4.73e-16	0.02 ± 0.26	2.14	···	> 26.00 F
24	622	J033250.2-274407	03 32 50.24	-27 44 7.58	15.70 ± 7.5	···	813.9(812.0)	9.23e-17	4.41e-17	<6.42e-16	···	−1.00 ± 0.00	2.34	2.29	24.20 ± 0.12 F
25	634	J033251.5-274746	03 32 51.47	-27 47 46.07	···	14.40 ± 6.2	820.3(841.4)	<6.08e-17	···	5.16e-16	2.22e-16	1.00 ± 0.00	2.17	1.72	24.86 ± 0.19 F
26	639	J033252.7-274240	03 32 52.70	-27 42 40.25	···	21.10 ± 9.3	459.8(456.7)	<1.63e-16	···	1.39e-15	6.14e-16	1.00 ± 0.00	2.34	0.36	23.36 ± 0.04 F
27	629	J033253.5-275104	03 32 53.48	-27 51 4.72	15.40 ± 6.1	···	831.6(844.0)	8.86e-17	3.51e-17	<5.13e-16	···	−1.00 ± 0.00	2.16	1.25	25.26 ± 0.12 F
28	628	J033255.4-275105	03 32 55.43	-27 51 5.33	15.00 ± 6.8	···	838.1(848.3)	8.56e-17	3.88e-17	<5.81e-16	···	−1.00 ± 0.00	2.29	···	> 26.76 F

[a] Optical cutout ID number, in order of RA

[b] Unique Detection ID

[c] IAU Registered Name, based on original (not offset) X–ray coordinates

[d] Right Ascension, offset from *Chandra* by $-1.2''$

[e] Declination, offset from *Chandra* by $0.8''$

[f] Net Counts in soft (0.5 - 2 keV) band

[g] Net Counts in hard (2 - 10 keV) band

[h] Effective exposure time in the soft(hard) band, in kiloseconds

[i] Flux in soft (0.5 - 2 keV) band, c.g.s. units

[j] Error on soft flux

[k] Flux in hard (2 - 10 keV) band, c.g.s. units

[l] Error on hard flux

[m] Hardness Ratio, defined as (H - S)/(H + S) where H and S are the net counts in the hard and soft bands respectively

[n] Error on the X-ray source position as calculated in the text, in arcseconds

[o] Separation of the candidate optical counterpart, in arcseconds

[p] Vega R magnitude for the optical counterpart in either the FORS (F) or WFI (W) filter

Table 4. Wavdetect Only

ID[a]	XID[b]	CXO CDFS[c]	RA (J2000)[d]	Dec (J2000)[e]	Soft Cts.[f]	Hard Cts.[g]	Exp Time[h]	Soft Flux[i]	Error[j]	Hard Flux[k]	Error[l]	HR[m]	Pos. Err.[n]	Sep.[o]	R[p]
1	645	J033150.0-274941	03 31 49.95	-27 49 41.74	66.50 ± 13	···	620.1(621.2)	4.62e-16	9.04e-17	<1.00e-15	···	-1.00 ± 0.00	1.86	1.83	21.00 ± 0.02 W
2	643	J033156.4-275257	03 31 56.43	-27 52 57.00	33.90 ± 10	28.90 ± 12.5	821.3(824.4)	1.97e-16	5.82e-17	1.06e-15	4.57e-16	-0.08 ± 0.26	2.05	···	> 26.10 W
3	124	J033202.6-274525	03 32 2.65	-27 45 25.20	14.80 ± 6.8	···	816.4(827.9)	8.67e-17	3.98e-17	<6.08e-16	···	-1.00 ± 0.00	2.30	0.49	25.49 ± 0.27 F
														1.32	25.29 ± 0.26 F
														2.20	24.94 ± 0.23 F
4	642	J033215.3-274159	03 32 15.35	-27 41 59.46	15.40 ± 7.5	25.60 ± 10	838.8(841.7)	8.78e-17	4.28e-17	9.17e-16	3.58e-16	0.25 ± 0.29	2.40	1.07	24.54 ± 0.25 F
5	649	J033224.9-273851	03 32 24.85	-27 38 51.54	21.80 ± 10.3	···	391.7(386.2)	2.15e-16	1.01e-16	<1.52e-15	···	-1.00 ± 0.00	2.57	···	> 25.72 F
6	651	J033228.6-275809	03 32 28.56	-27 58 9.95	44.60 ± 10.9	···	361.3(353.8)	4.16e-16	1.02e-16	<1.37e-15	···	-1.00 ± 0.00	2.00	1.29	18.97 ± 0.01 W
7	641	J033239.1-275917	03 32 39.15	-27 59 17.81	30.50 ± 11.2	39.00 ± 14.4	250.6(243.5)	4.10e-16	1.51e-16	3.40e-15	1.26e-15	0.14 ± 0.26	2.37	···	> 26.10 W
8	646	J033245.2-274724	03 32 45.21	-27 47 24.90	17.10 ± 6.2	···	893.5(918.7)	9.15e-17	3.32e-17	<4.48e-16	···	-1.00 ± 0.00	1.98	0.30	21.01 ± 0.01 F
9	644	J033246.0-275746	03 32 45.96	-27 57 46.76	32.80 ± 11.4	···	439.6(431.2)	3.36e-16	1.17e-16	<1.56e-15	···	-1.00 ± 0.00	2.26	1.17	16.74 ± 0.00 W
10	648	J033246.6-275716	03 32 46.58	-27 57 16.06	46.40 ± 12.7	···	687.6(676.6)	3.23e-16	8.83e-17	<1.10e-15	···	-1.00 ± 0.00	2.06	···	> 26.10 W
11	652	J033249.4-274301	03 32 49.35	-27 43 1.31	20.80 ± 8.6	···	806.3(793.3)	1.23e-16	5.10e-17	<7.37e-16	···	-1.00 ± 0.00	2.25	1.81	20.64 ± 0.01 F
12	647	J033301.9-275009	03 33 1.95	-27 50 9.17	26.80 ± 8.6	···	750.8(755.0)	1.71e-16	5.48e-17	<7.32e-16	···	-1.00 ± 0.00	2.08	0.94	18.51 ± 0.01 W
13	653	J033303.8-274411	03 33 3.78	-27 44 11.18	···	25.90 ± 10.4	282.7(281.1)	<1.72e-16	···	1.81e-15	7.25e-16	1.00 ± 0.00	2.32	1.12	25.04 ± 0.25 F
														1.82	26.20 ± 0.39 F
14	650	J033307.4-274433	03 33 7.38	-27 44 33.22	27.60 ± 9.5	···	259.9(257.0)	3.30e-16	1.14e-16	<1.55e-15	···	-1.00 ± 0.00	2.23	0.40	17.40 ± 0.00 F

[a]Optical cutout ID number, in order of RA

[b]Unique Detection ID

[c]IAU Registered Name, based on original (not offset) X–ray coordinates

[d]Right Ascension, offset from *Chandra* by $-1.2''$

[e]Declination, offset from *Chandra* by $0.8''$

[f]Net Counts in soft (0.5 - 2 keV) band

[g]Net Counts in hard (2 - 10 keV) band

[h]Effective exposure time in the soft(hard) band, in kiloseconds

[i]Flux in soft (0.5 - 2 keV) band, c.g.s. units

[j]Error on soft flux

[k]Flux in hard (2 - 10 keV) band, c.g.s. units

[l]Error on hard flux

[m]Hardness Ratio, defined as (H - S)/(H + S) where H and S are the net counts in the hard and soft bands respectively

[n]Error on the X-ray source position as calculated in the text, in arcseconds

[o]Separation of the candidate optical counterpart, in arcseconds

[p]Vega R magnitude for the optical counterpart in either the FORS (F) or WFI (W) filter

Table 5. Extended Sources

XID	RA (J2000)	Dec (J2000)	Soft Cts	Soft Flux	S/N_{soft}	FWHM($''$)	Off-axis Angle($'$)
37	3 32 32.21	-27 41 56.22	89.8	5.03e-16	8.0	5.6	6.77
116	3 32 30.07	-27 44 5.35	93.0	5.29e-16	8.8	3.9	4.58
132	3 32 44.09	-27 54 56.12	40.9	2.19e-16	4.8	6.9	7.17
138	3 32 50.11	-27 41 35.30	51.8	9.13e-16	5.9	7.3	8.54
147	3 32 46.43	-27 46 32.74	25.9	1.49e-16	4.0	4.1	4.50
240	3 32 59.20	-27 51 40.43	43.8	2.46e-16	4.9	7.4	7.43
249	3 32 19.49	-27 54 6.55	27.4	1.46e-16	3.7	8.2	5.80
507	3 33 0.12	-27 49 25.50	23.3	1.43e-16	3.0	5.7	7.04
511	3 32 36.63	-27 46 31.30	22.6	1.27e-16	3.5	5.8	2.79
514	3 32 33.56	-27 43 12.40	27.1	1.57e-16	4.1	5.0	5.56
522	3 32 21.50	-27 55 50.99	68.2	3.78e-16	6.6	6.1	7.36
527	3 32 18.59	-27 54 14.40	36.6	1.97e-16	4.4	6.6	6.00
529	3 32 16.32	-27 55 25.97	23.4	1.32e-16	3.0	9.0	7.29
544	3 31 54.64	-27 51 4.75	34.7	1.90e-16	3.9	6.5	7.86
560	3 32 6.27	-27 45 38.02	23.2	1.26e-16	3.6	5.5	5.77
566	3 32 18.11	-27 47 19.50	30.9	2.33e-16	4.5	3.4	2.65
581	3 32 7.47	-27 49 43.68	17.6	9.51e-17	3.0	3.8	4.77
594	3 32 9.83	-27 42 49.68	237.0	1.36e-15	12.0	8.1	7.14
645	3 32 49.95	-27 49 41.74	262.1	1.75e-15	9.0	···	8.58

Fig. 1.— Soft(0.5–2 keV) band image of 942 ks exposure of the CDFS. The image is smoothed with a Gaussian with $\sigma = 1''$.

Fig. 2.— Hard (2–7 keV) band image of 942 ks exposure of the CDFS. The image is smoothed with a Gaussian with $\sigma = 1''$.

Fig. 3.— Exposure map of the combined 11 exposures of the CDFS, computed for an energy of 1.5 keV.

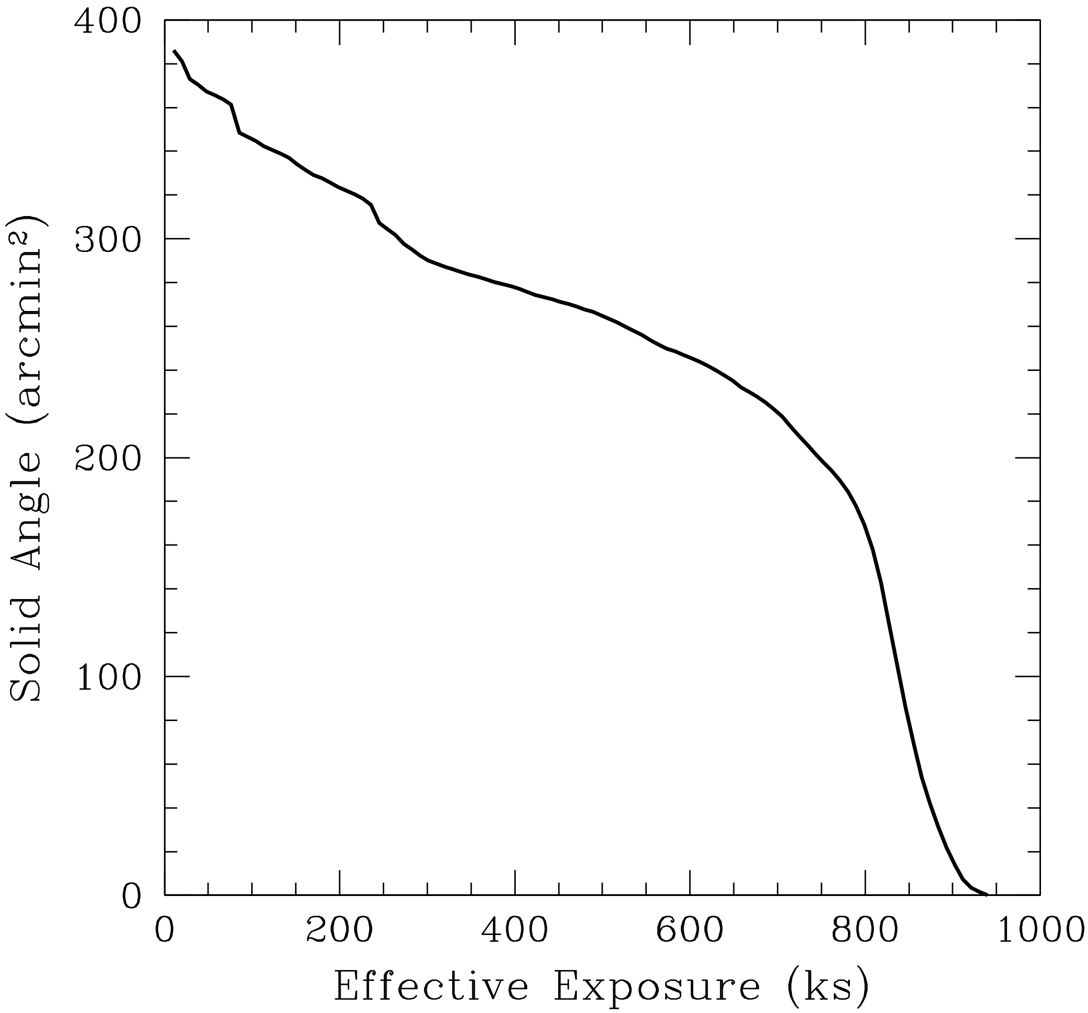

Fig. 4.— Solid angle as a function of the effective exposure time in the soft band.

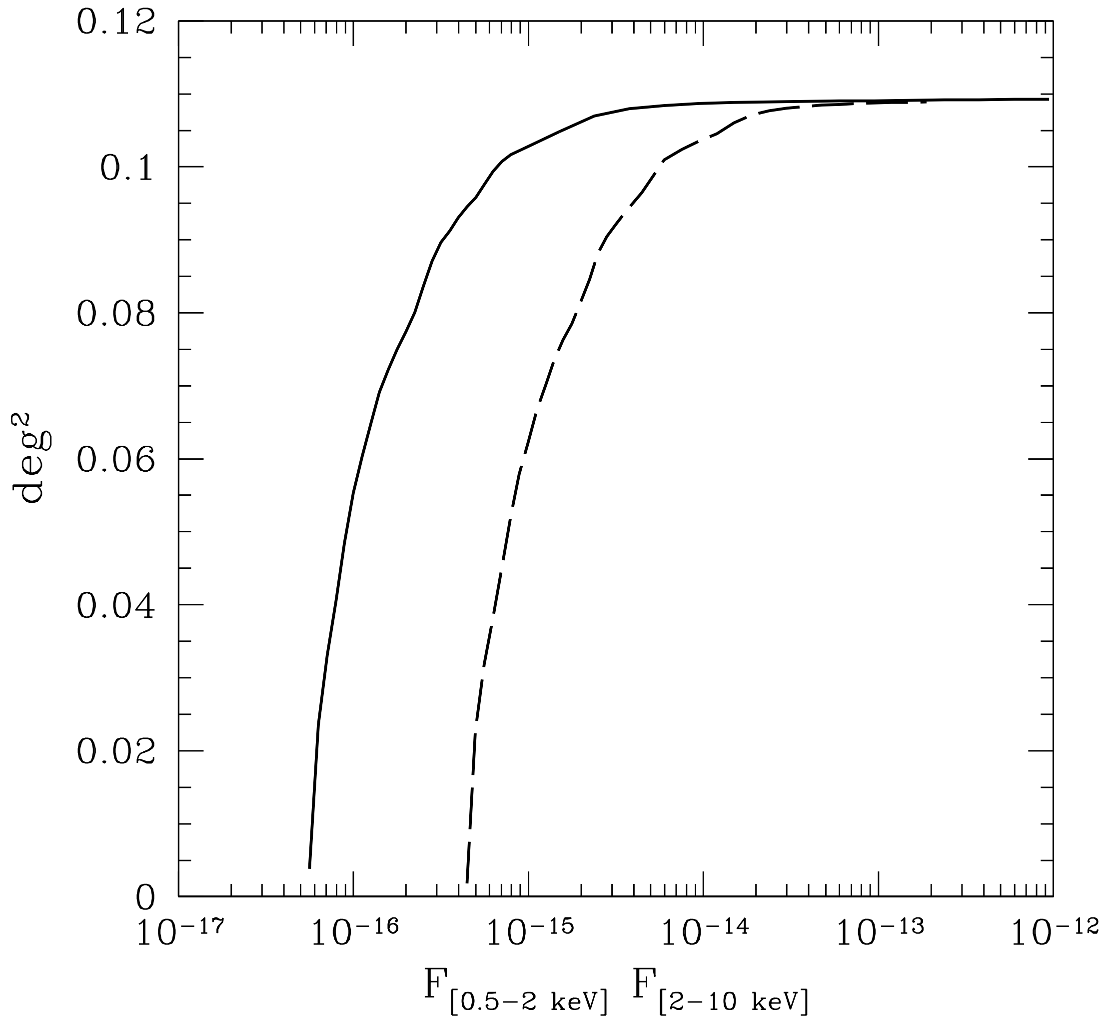

Fig. 5.— The sky coverage (area covered vs. flux limit) for the soft image (solid line) and the hard image (dashed line). The sky coverage is plotted against the 2–10 keV energy flux which is actually used in the catalog.

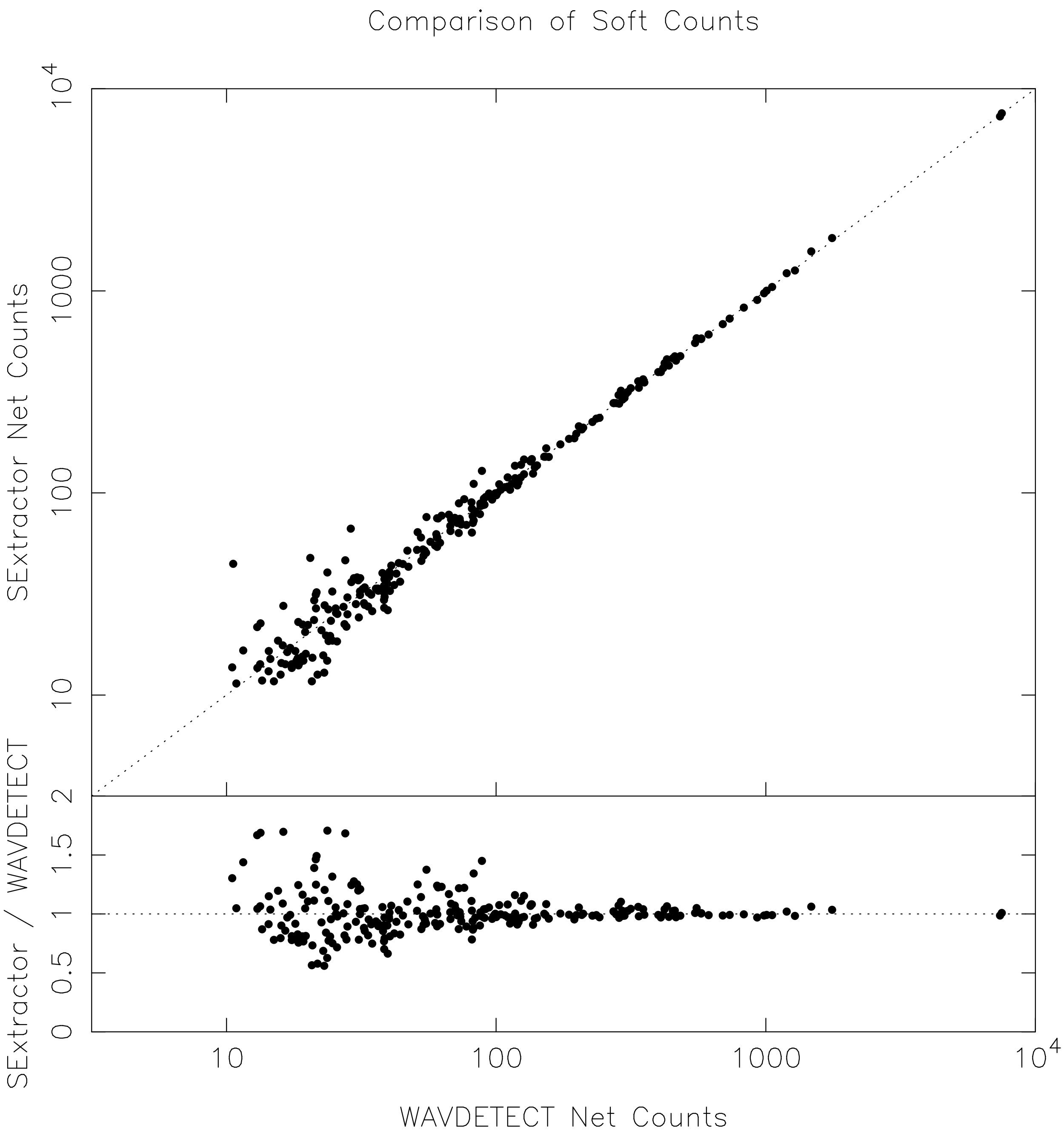

Fig. 6.— Comparison between the photon counts obtained with the SExtractor method and those obtained with the WAVDETECT method for the sources detected in the 0.5-2 keV band.

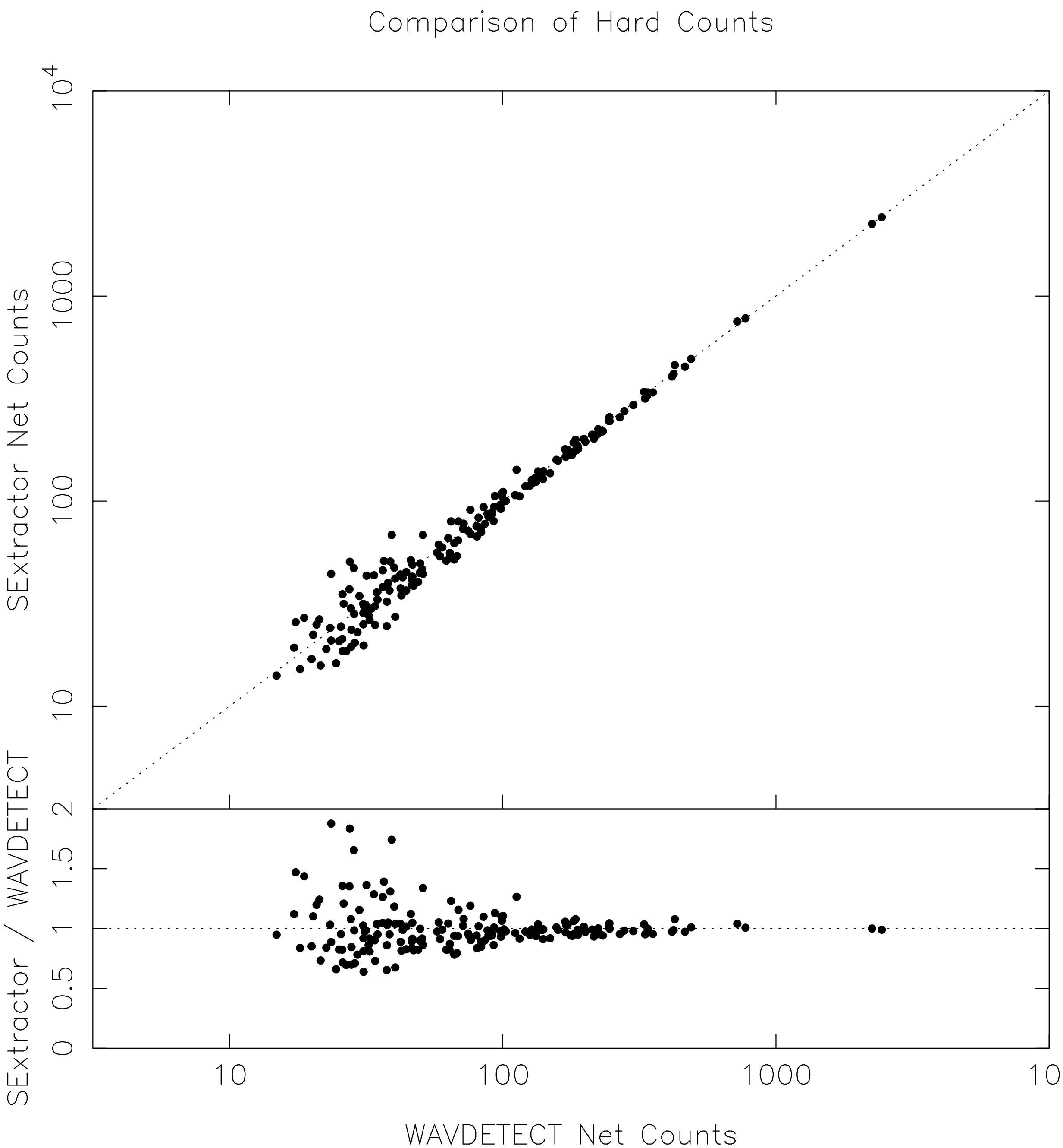

Fig. 7.— The same as in Fig. 6 but for the sources detected in the 2–7 keV band

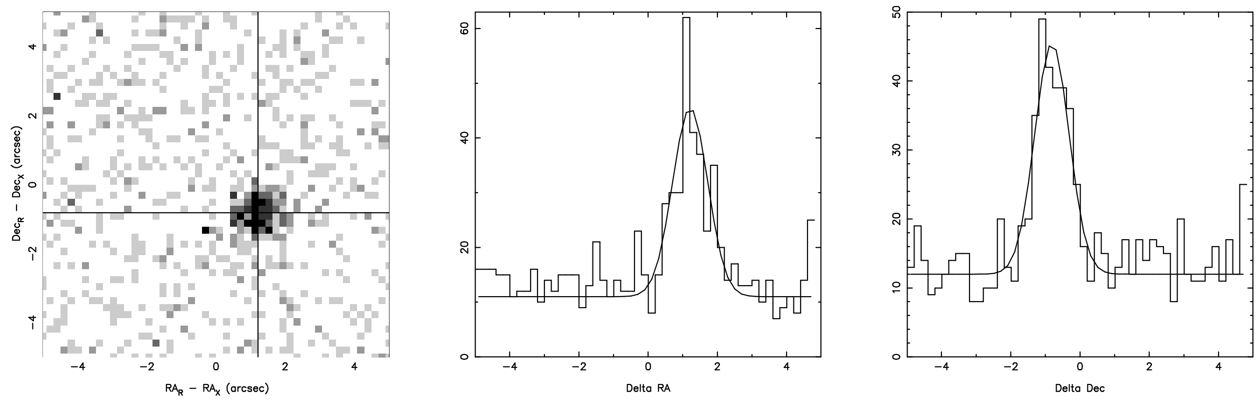

Fig. 8.— Coordinate offsets between *Chandra* and FORS R. The 2D histogram shows the correlation peak between the two catalogs. Each 1D distribution was fit with a Gaussian to determine both the mean and scatter of the coordinate offsets.

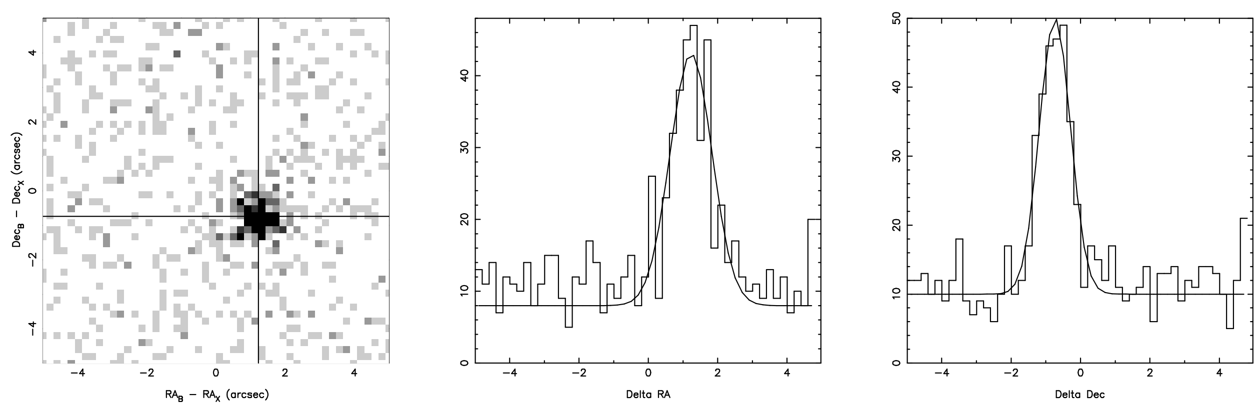

Fig. 9.— Coordinate offsets between *Chandra* and WFI R. Identical to Figure 8.

Fig. 10.— Selection of extended sources in the FWHM vs off–axis angle plane. Top panel: Crosses are sources in CDFS (with S/N > 3 in the soft band), diamonds are sources drawn from two additional archival deep Chandra fields. The solid line is a parabolic best fit to the PSF, dashed and dot-dashed lines are the 3σ and 2σ limits of the FWHM distribution respectively (see text). Filled dots are sources which are likely to be extended. Bottom panel: distribution of residuals for the CDFS sources only, after subtracting the PSF fit model.

Fig. 11.— K–band image of source XID 645, one of the extended low surface–brightness sources in the CDFS. The image is from the EIS data of the CDFS (Vandame et al. 2001) with overlaid Chandra contours corresponding to $[2, 3, 5, 7, 15]\sigma$ above the local background. The soft band image smoothed with a $\sigma = 5''$ Gaussian was used.

Fig. 12.— R–band FORS mosaic image of the brightest extended source in the CDFS (XID 594, identified as a poor cluster at $z = 0.72$) with overlaid *Chandra* contours corresponding to $[2, 4, 5, 7, 10, 15, 200]\sigma$ above the local background. The soft band image smoothed with a $\sigma = 2.5''$ Gaussian was used (upper left inset).

Fig. 13.— f_X vs. f_R for the CDFS sample. We computed the energy flux f_X in the 0.5–10 keV band. The circles and squares indicate sources detected in only the soft or hard band respectively. The arrows indicate lower limit in the magnitude of optically undetected sources. The differences in these lower limits reflects the different depth reached by the FORS images, from where the R magnitueds were derived. The three dashed lines are lines of constant f_X/f_R, with values left to right of 0.1, 1 and 16.

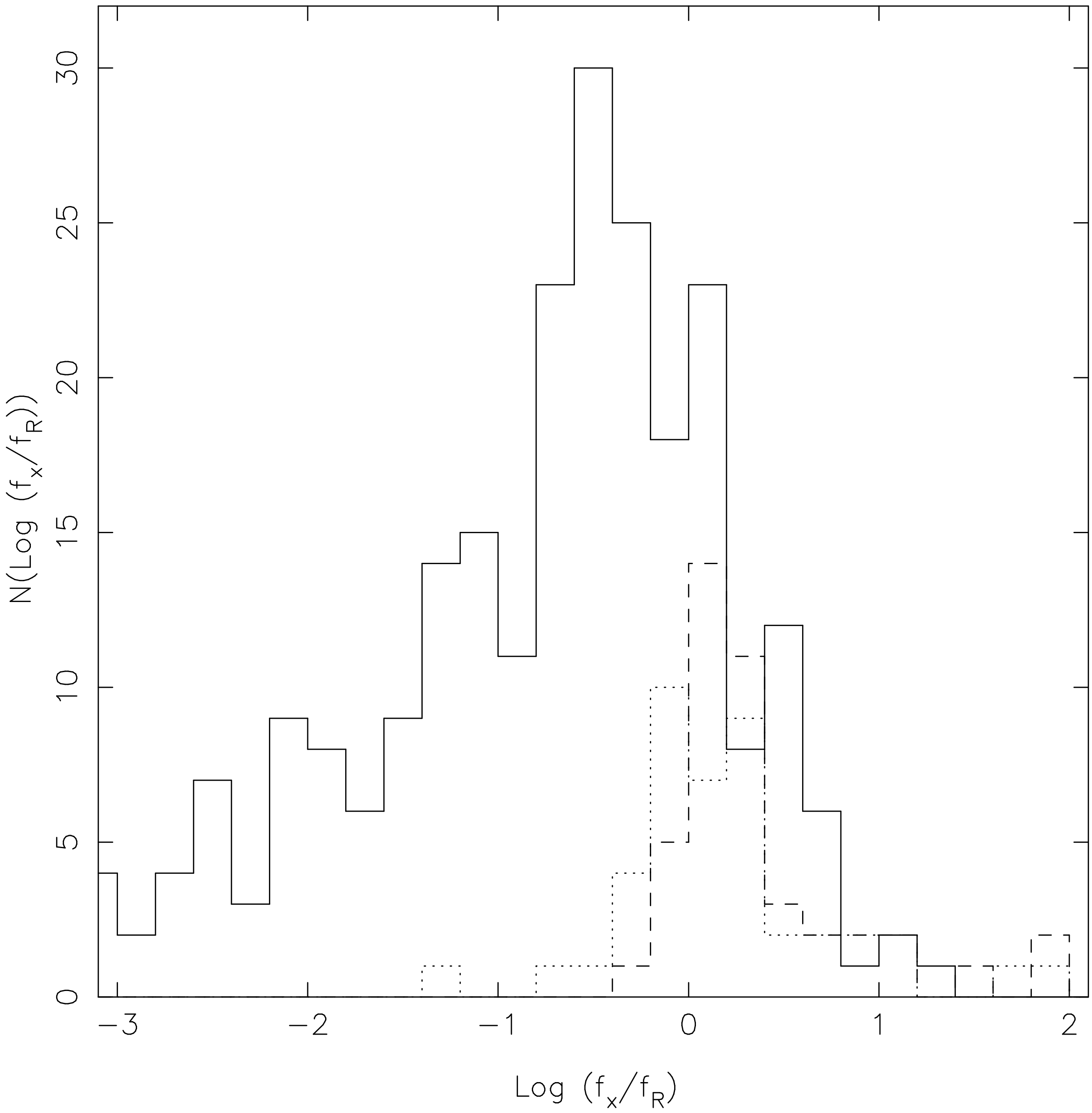

Fig. 14.— The distribution of Log f_X/f_R for the current sample. The solid line histogram is for the CDFS data, the dotted line is the *ROSAT* Lockman Hole data (Schmidt et al. 1998) and the dashed line is upper limits in the CDFS/FORS1 dataset for the optically undetected counterparts (arrows in Figure 13).

Fig. 15.— Optical cutouts for the Main Catalog. ID number (XID in parenthesis) and optical band is printed in the upper left corner of each image. The energy flux in the soft band is in the lower left, while the flux in the hard 2–10 keV band is in the lower right. The iso-intensity contours are at 3, 5, 10, 20 and 100 sigma above the local background. The box indicates an optical counterpart candidate. The 3σ positional error (after the relation in §4.1) is indicated by the circle in the center. Each cutout is 20 arcsec wide.

Fig. 16.— Optical cutouts for the SExtractor Only Catalog. ID number (XID in parenthesis) and band is printed in the upper left corner of each image. The energy flux in the soft band is in the lower left, while the flux in the hard 2–10 keV band is in the lower right. The iso–intensity contours are at 2, 5, 10 and 20 sigma above the background. The box indicates an optical counterpart candidate. The positional error is indicated by the circle in the center.

Fig. 17.— Optical cutouts for the WAVDETECT Only Catalog. ID number (XID in parenthesis) and band is printed in the upper left corner of each image. The energy flux in the soft band is in the lower left, while the flux in the hard 2–10 keV band is in the lower right. The iso-intensity contours are at 2, 5, 10 and 20 sigma above the background. The box indicates an optical counterpart candidate. The positional error is indicated by the circle in the center.

This figure "figure2.jpg" is available in "jpg" format from:

http://arXiv.org/ps/astro-ph/0112184v1

This figure "figure3.jpg" is available in "jpg" format from:

http://arXiv.org/ps/astro-ph/0112184v1

This figure "figure13.jpg" is available in "jpg" format from:

http://arXiv.org/ps/astro-ph/0112184v1

This figure "figure15e.jpg" is available in "jpg" format from:

http://arXiv.org/ps/astro-ph/0112184v1

This figure "figure15h.jpg" is available in "jpg" format from:

http://arXiv.org/ps/astro-ph/0112184v1

This figure "figure15r.jpg" is available in "jpg" format from:

http://arXiv.org/ps/astro-ph/0112184v1